QCD corrections to heavy-quark production in $p\bar{p}$ collisions

W. Beenakker, H. Kuijf, and W. L. van Neerven
Instituut Lorentz, University of Leiden, P.O. Box 9506, 2300 RA, Leiden, The Netherlands

J. Smith*
Institute for Theoretical Physics, State University of New York at Stony Brook, Stony Brook, New York 11794-3840
(Received 16 August 1988)

We investigate QCD corrections to the cross section and differential distributions for $p+\bar{p}\to Q+\bar{Q}+X$, where Q and $\bar{Q}$ are heavy quarks. We calculate the order-α_s corrections to the parton reaction $g+g\to Q+\bar{Q}$. At the quark level this involves the computation of the virtual-gluon contributions to the reactions $g+g\to Q+\bar{Q}$, and the soft and hard contributions from the reaction $g+g\to Q+\bar{Q}+g$. Results are given for the cross section and differential distributions for the range of $p\bar{p}$ collision energies available at CERN and Fermilab. A comparison is made with the recent data from the UA1 Collaboration.

I. INTRODUCTION

During the last few years heavy-flavor production in hadronic collisions has become an important subject.[1] New experimental results have come from the search for the top quark and the study of the properties of bottom and charmed quarks.[2] Analysis of the ratio $\sigma(p+\bar{p}\to\mu^{\pm}+\mu^{\pm}+X)/\sigma(p+\bar{p}\to\mu^{+}+\mu^{-}+X)$ (Ref. 3) established the phenomenon of $B^0\bar{B}^0$ mixing,[4] and allowed bounds to be placed on the Kobayashi-Maskawa[5] matrix elements involving the top quark. The new experimental data allows theorists to test the application of perturbative QCD (Refs. 6–8) to processes where heavy quarks are produced via light parton-parton interactions. This is a subject of considerable importance for future pp and $p\bar{p}$ accelerators.

There are two important contributions to heavy-flavor production. The first one, which is theoretically as well as experimentally better understood, is the process where the heavy flavors appear as the decay products of the W and Z bosons. The latter are produced via the Drell-Yan mechanism in $p\bar{p}$ collisions. However, this source of heavy-flavor production is only important for the top quark[9] provided its mass satisfies the relation $m_t<M_Z/2$ or $m_t<M_W-m_b$. In the second and dominant mechanism the heavy quarks are directly created via parton-parton collisions. When the heavy quarks are produced at large transverse momentum this process can be described by perturbative QCD, as will be explained below. In lowest order of the strong coupling constant g, there are two parton-parton subprocesses, quark-antiquark annihilation and gluon-gluon fusion, i.e.,

$$q+\bar{q}\to Q+\bar{Q}\ , \tag{1.1}$$

and

$$g+g\to Q+\bar{Q}\ . \tag{1.2}$$

Both lowest-order $O(\alpha_s^2)$ processes have been extensively analyzed in the literature.[10,11] This analysis reveals that at energies just above the threshold the total cross section for process (1.1) is much larger than that for (1.2), provided the incoming quarks are valence quarks, which happens to be the case in $p\bar{p}$ collisions. When the c.m. energy is increased so that it is much larger than the heavy-quark mass then the cross section for the gluon-gluon-fusion process is the dominant one. The cross section for (1.2) can be as much as an order of magnitude larger than that for (1.1).

If one looks at the differential cross section one observes that both reactions produce the heavy quarks mainly in the center of the (pseudo)rapidity region.[3,12] Furthermore, the average transverse momentum of the heavy quark is proportional to its mass.[3,12] It is of interest to see how these features of the Born cross section are modified by higher-order radiative corrections or by inclusion of new production mechanisms which are present in higher order in α_s. Up to order α_s^3 this requires an examination of the cross sections and differential distributions for the following parton-parton processes:[13,14]

$$q+\bar{q}\to Q+\bar{Q}+g\ , \tag{1.3}$$

$$g+g\to Q+\bar{Q}+g\ , \tag{1.4}$$

and

$$g+q(\bar{q})\to Q+\bar{Q}+q(\bar{q})\ . \tag{1.5}$$

In a recent paper[13] the total cross sections of the above processes have been completely calculated. From this we infer that the radiative corrections are large and the main contribution to the order-α_s^3 cross section can be attributed to process (1.4). This is especially true when the heavy flavors are produced near threshold. In the limit $s\to 4m^2$ the phase space behaves like $\sqrt{s-4m^2}$ and the square of the Born amplitude is regular at $s=4m^2$. Hence the $O(\alpha_s^2)$ Born cross section vanishes at threshold. The $O(\alpha_s^3)$ contribution contains a Coulomb singularity caused by the exchange of massless gluons between the

massive quarks. The virtual matrix elements therefore contain terms of the type $\pi^2/\sqrt{s-4m^2}$, which, when combined with the phase-space factor $\sqrt{s-4m^2}$, yields a total cross section which approaches a constant. Hence, in the threshold region, the higher-order contributions are larger than those of the Born processes in (1.1) and (1.2).

As has been argued in Refs. 15–17 the gluon-gluon-fusion reaction (1.4) becomes even more important if one looks at the differential cross section with respect to the transverse momenta. At large transverse momenta one gets a sizable contribution to the differential cross section from the subprocess $g+g\to g+g^*$. Here g^* denotes the virtual gluon which decays into the heavy quarks. Usual QCD estimates give $d\sigma(g+g^*\to g+g)/d\sigma(g+g\to Q+\bar{Q})$ of the order of 100 and thus the contribution of the order-α_s correction overwhelms the cross section for the Born process by a large factor. However, this argument only holds if g^* is almost real, which is the case for charm production but not for b- or t-quark production. For this reason and the observation made above about the threshold enhancement we concentrate entirely on the gluon-gluon-fusion mechanism in this paper.

The presentation is organized as follows. In Sec. II we discuss the Born cross section and introduce the notation needed in the subsequent sections of the paper. We set up the notation in the most general way so that also the cross section for gluino-gluino production[17] $g+g\to\tilde{g}+\tilde{g}$ and the conventional QED reaction[18] $\gamma+\gamma\to e^++e^-$ can be calculated. In Sec. III we discuss the virtual corrections to process (1.2) and various details of our renormalization scheme. We use n-dimensional regularization throughout the paper.[19] In Sec. IV we give an outline of the calculation of process (1.4) and present a method of how to split the cross section into hard- and soft-gluon parts. The soft-gluon cross section will be given in Sec. V. In Sec. VI we discuss the mass factorization[20] of the hard and soft plus virtual parton cross sections. An explicit formula for the latter contribution will be presented. Also we indicate how one can reconstruct the unrenormalized virtual cross section from the soft plus virtual correction. In Sec. VII the results for the hadronic cross section will be presented and discussed. In Appendix A we list the scalar integrals which emerge from the calculation of the virtual matrix elements. Some kinematical details are presented in Appendix B. In Appendix C we list the angular integrals which appear in the two- to three-body reactions (1.3)–(1.5). Finally, in Appendix D, we present some of the longer formulas for the contributions of the soft plus virtual corrections.

II. THE BORN CROSS SECTION

As has been explained in the Introduction heavy-flavor production is dominated by the gluon-gluon-fusion process given in (1.1). The momentum assignment of this reaction will be denoted as

$$g(k_1)+g(k_2)\to Q(p_1)+\bar{Q}(p_2)\ . \tag{2.1}$$

The graphs which contribute to the Born amplitude are shown in Fig. 1. For the kinematical variables we choose

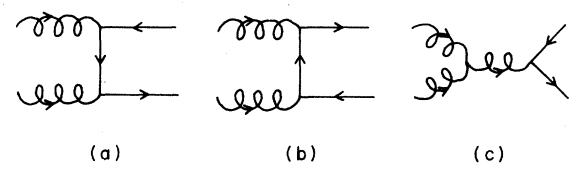

FIG. 1. The lowest-order Feynman diagrams contributing to the amplitude for the reaction $g(k_1)+g(k_2)\to Q(p_1)+\bar{Q}(p_2)$.

$$\begin{aligned} s&=2k_1\cdot k_2\ ,\\ t_1&\equiv t-m^2=(k_1-p_1)^2-m^2\ ,\\ u_1&\equiv u-m^2=(k_1-p_2)^2-m^2\ . \end{aligned} \tag{2.2}$$

The Born matrix element, which will be denoted by $M^B_{\mu\nu}$, is given by the standard QCD Feynman rules. In this and the subsequent sections we want to keep the notation as general as is possible. This enables us to describe processes which are related to the one given in (2.1) including also their radiative corrections. The two examples are the standard QED electron-positron pair creation

$$\gamma(k_1)+\gamma(k_2)\to e^-(p_1)+e^+(p_2) \tag{2.3}$$

and gluino pair production

$$g(k_1)+g(k_2)\to\tilde{g}(p_1)+\tilde{g}(p_2)\ , \tag{2.4}$$

whose amplitudes can be obtained from the results of Ref. 17.

Since the cross sections for the Born process and its radiative corrections have to be evaluated in n dimensions the algebra was performed by using the program SCHOONSCHIP (Ref. 21). However, this program is only suitable for four-dimensional γ-matrix algebra so we had to adapt the program for our n-dimensional computations.

The square of the Born amplitude $M^B\equiv\epsilon^\mu(k_1)\epsilon^\nu(k_2)M^B_{\mu\nu}$ summed over the initial polarizations and final spins can be written as

$$\sum M^B M^{B*}=2g^4(C_O B_O+C_K B_K+C_{\rm QED}B_{\rm QED})\ , \tag{2.5}$$

with B_O, B_K related to $B_{\rm QED}$ by

$$B_O=\left[1-2\frac{t_1u_1}{s^2}\right]B_{\rm QED},\quad B_K=-B_{\rm QED}\ , \tag{2.6}$$

where $B_{\rm QED}$ is given by

$$B_{\rm QED}=\frac{t_1}{u_1}+\frac{u_1}{t_1}+\frac{4m^2s}{t_1u_1}\left[1-\frac{m^2s}{t_1u_1}\right]+\epsilon\left[-1+\frac{s^2}{t_1u_1}\right]+\epsilon^2\frac{s^2}{4t_1u_1}\ , \tag{2.7}$$

and $\epsilon=n-4$. Notice that the epsilon terms are mass independent. The color factors C_O, C_K, and $C_{\rm QED}$ are different for the various processes listed above. They are given by

$$C_O=N(N^2-1),\quad C_K=(N^2-1)N^{-1},\quad C_{\rm QED}=0\ ,$$
$$C_O=0,\quad C_K=0,\quad C_{\rm QED}=4\ , \tag{2.8}$$
$$C_O=2N^2(N^2-1),\quad C_K=-2N^2(N^2-1),\quad C_{\rm QED}=0\ ,$$

for reactions (2.1), (2.3), and (2.4), respectively, where N denotes the number of colors.

In order to avoid the introduction of external ghost lines while summing over the gluon helicities we limit ourselves to the sum over the physical polarizations of the gluon and use

$$P_i^{\mu\nu}\equiv\sum_T \epsilon_T^{\mu}(k_i)\epsilon_T^{\nu}(k_i)$$
$$=-g^{\mu\nu}+\frac{n_i^{\mu}k_i^{\nu}+k_i^{\mu}n_i^{\nu}}{n_i\cdot k_i}-\frac{n_i^2k_i^{\mu}k_i^{\nu}}{(n_i\cdot k_i)^2}\ . \tag{2.9}$$

$\sum_T$ denotes the sum over the transverse polarizations of gluon i ($i=1,2$) and the polarization tensor $P_i^{\mu\nu}$ satisfies the relations

$$k_{i\mu}P_i^{\mu\nu}=P_i^{\mu\nu}k_{i\nu}=0,\quad n_{i\mu}P_i^{\mu\nu}=P_i^{\mu\nu}n_{i\nu}=0\ . \tag{2.10}$$

We have chosen an arbitrary vector n_i ($n_i^2\neq 0$) for each gluon i with $n_1\neq n_2$. Since the expression in (2.4) is gauge invariant the explicit dependence on n_i drops out. Therefore this method serves as a check on the gauge invariance of the physical quantities calculated in this paper. Note however that we have taken the Feynman gauge for the internal gluon propagator which appears in the Born amplitude. The same gauge will be chosen for the calculation of the higher-order radiative corrections which will be discussed in the subsequent sections. The independence of the matrix element squared on the n_i corresponding to the external gluons is a consequence of the Slavnov-Taylor identities.[22] We will say more about this in the next sections.

Averaging over the initial gluon polarizations and color we find that the result for the Born cross section in n dimensions can be expressed as

$$s^2\frac{d^2\sigma_{gg}^{(0)}}{dt_1du_1}=\tfrac{1}{4}K\frac{\pi S_\epsilon}{\Gamma(1+\epsilon/2)}\left[\frac{t_1u_1-sm^2}{\mu^2 s}\right]^{\epsilon/2}$$
$$\times\delta(s+t_1+u_1)\sum M^B M^{B*}\ , \tag{2.11}$$

where K is the color-average factor. In the case of processes (2.1) and (2.2) it is given by

$$K=(N^2-1)^{-2}\ , \tag{2.12}$$

while, for the QED process (2.3),

$$K=1\ . \tag{2.13}$$

The mass parameter μ in (2.11) originates from the dimensionality of the gauge-coupling constant g in n dimensions. The constant $S_\epsilon=(4\pi)^{-2-\epsilon/2}$ originates from the n-dimensional integration over the solid angle and the remaining factor comes from the two-particle-to-two-particle phase-space integral. For later purposes we will split the Born cross section in the same way as has been done for the matrix element squared in (2.5). Using a shorthand notation we can write

$$d\sigma_{gg}^{(0)}=d\sigma_{gg,O}^{(0)}+d\sigma_{gg,K}^{(0)}+d\sigma_{gg,\rm QED}^{(0)}\ , \tag{2.14}$$

where the three cross sections on the right-hand side of (2.14) can be derived from (2.5)–(2.8) and (2.11).

III. VIRTUAL CORRECTIONS

The order-α_s QCD corrections to the differential cross section in (2.11) require the calculation of the Feynman diagrams shown in Fig. 2. The ultraviolet (UV), infrared (IR), and the collinear or mass (M) singularities which appear in the graphs are regularized by n-dimensional regularization. In order to simplify the calculations we have treated the heavy (c,b,t) and light (u,d,s) quarks in the same way by giving both of them a mass m_f. Note, however, that in the light-quark case m_f has to be considered as a regulator for the collinear divergence which will eventually be removed by mass factorization.

For the internal gluon propagators we have chosen the Feynman gauge. Although n-dimensional regularization preserves the Slavnov-Taylor identities[22] we have explicitly checked them on the amplitude level in our calculation. The relations for the four-, three-, and two-point functions can be found in the above reference. This ensures that the total virtual amplitude denoted by $M_{\mu\nu}^V$ satisfies the identity (see Fig. 3)

$$k_1^{\mu}M_{\mu\nu}^V(k_1,k_2)=M_{\nu}^{gh}(k_1,k_2)\ , \tag{3.1}$$

provided the external gluon and quark legs are put on their renormalized mass shells. Notice that the ghost-ghost–quark-antiquark amplitude $M_{\nu}^{gh}(k_1,k_2)$ is proportional to $k_{2\nu}$.

The computation of $M_{\mu\nu}^V$ has been done as follows. For the Lorentz algebra we used the program SCHOONSCHIP (Ref. 21). The Feynman integrals which contain loop momenta in the numerator have been dealt with by using an adapted version of the reduction program of Passarino and Veltman.[23] This program, which was originally designed to treat the UV divergences in a proper way, has to be extended to account for the IR and M singularities. This can be attributed to the appearance of double-pole terms ϵ^{-2} which show up when IR and M singularities coincide. In this way we could reduce all Feynman integrals to a set of elementary scalar integrals which are listed in Appendix A. These scalar integrals have been computed in two different ways. The first one is via the standard Feynman parametrization technique. This is feasible because many particles in the loop graphs are either massless or have only UV divergences. The second calculation proceeds via the computation of the absorptive part of the Feynman integrals by application of the Cutkosky rules in n dimensions. The real part is then obtained by using the technique of dispersion relations.[24]

The virtual cross section is obtained from the interference term between the virtual and the Born amplitude. Summing over the initial-gluon polarizations and the final spins this term will be denoted by

$$\sum(M^V M^{B*}+M^B M^{V*}) \tag{3.2}$$

with $M^V\equiv\epsilon^{\mu}(k_1)\epsilon^{\nu}(k_2)M_{\mu\nu}^V$. If we now use the polarization sum $P_i^{\mu\nu}$ in (2.9) the identity in (3.1) implies that ex-

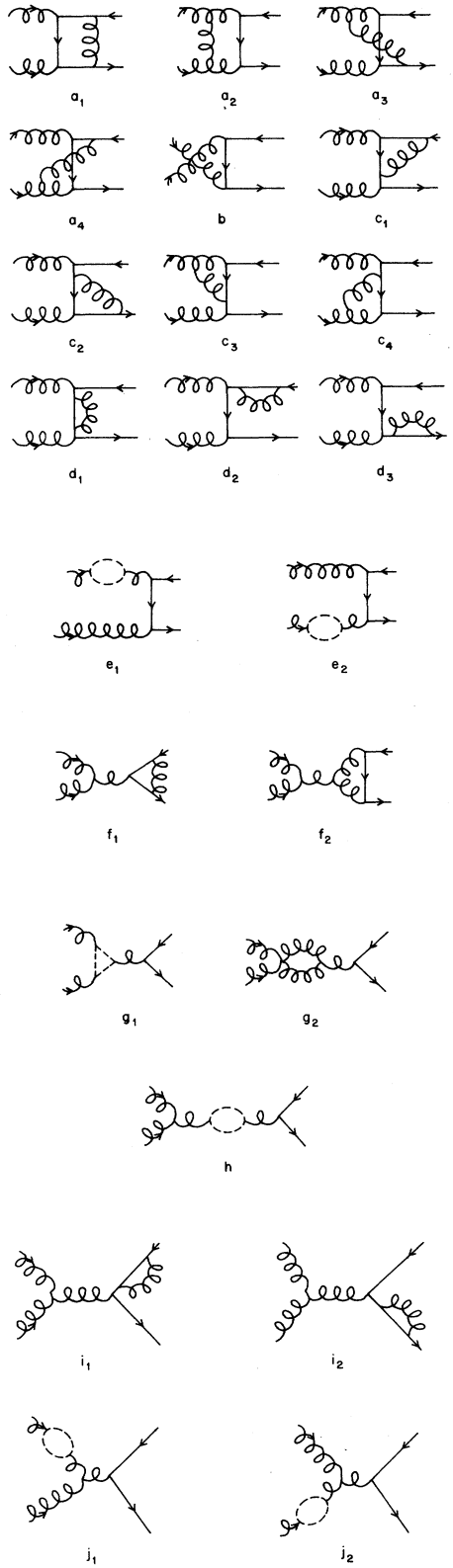

FIG. 2. The order-g^2 Feynman diagrams contributing to the amplitude for the reaction $g(k_1)+g(k_2)\to Q(p_1)+\bar{Q}(p_2)$. Additional graphs are obtained from a_1-a_2; c_1-c_4; d_1-d_3; e_1-e_2 by reversing the arrows on the external fermion lines. Loops with dotted lines represent quark, gluon, and ghost loops.

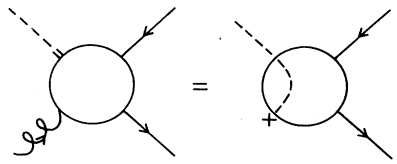

FIG. 3. Diagrammatic representation of the Slavnov-Taylor identity for the process $g+g\to Q+\bar{Q}$. For an explanation of the signs see Ref. 22.

pression (3.2) is gauge invariant and therefore independent of n_i. This we have checked by using an arbitrary n_i. The final result for (3.2) can be written in the same way as we have done for the Born amplitude in (2.5):

$$\sum (M^V M^{B*}+M^B M^{V*}) = g^6(NC_O V_O + NC_K V_K + \bar{C}_{\rm QED} V_{\rm QED} + C_O V_f) \ . \tag{3.3}$$

This formula can be applied to the virtual corrections to (2.1), (2.3), and (2.4) with C_O and C_K defined in (2.8). However, the color factor for QED is now different so we use $\bar{C}_{\rm QED}$ with

$$\bar{C}_{\rm QED}=\frac{N^4-1}{N^2}, \quad \bar{C}_{\rm QED}=8, \quad \bar{C}_{\rm QED}=0 \ , \tag{3.4}$$

for (2.1), (2.3), and (2.4), respectively. V_f denotes the fermion-loop contributions to the three-gluon vertex and the gluon self-energy. Here the sum over all flavors is implicitly understood. The expressions for V_O, V_K, $V_{\rm QED}$, and V_f are rather lengthy so that they will not be given here. However, they can be easily reconstructed from the reduced virtual and soft cross section. How to do this will be shown in Sec. VI after we have performed mass factorization. The virtual unrenormalized cross section becomes

$$s^2\left[\frac{d^2\sigma_{gg}^{(1)}}{dt_1 du_1}\right]^V = \frac{1}{4}\frac{\pi S_\epsilon}{\Gamma(1+\epsilon/2)}K\left[\frac{t_1u_1-sm^2}{\mu^2 s}\right]^{\epsilon/2} \times \delta(s+t_1+u_1)\sum (M^V M^{B*}+M^B M^{V*}), \tag{3.5}$$

where K is defined in (2.12) and (2.13). Using the same shorthand notation as in (2.14) we can split the virtual cross section as follows:

$$(d\sigma_{gg}^{(1)})^V=(d\sigma_{gg,O}^{(1)})^V+(d\sigma_{gg,K}^{(1)})^V+(d\sigma_{gg,\rm QED}^{(1)})^V +(d\sigma_{gg,f}^{(1)})^V \ . \tag{3.6}$$

In the explicit expression for the virtual cross section we observe single- and double-pole terms of the type ϵ^{-i} $(i=1,2)$ which are due to the UV, IR, and M singularities. Double-pole terms only appear when IR and M singularities coincide. The latter show up only in the O and K part of the virtual cross section in (3.6). The QED part has no collinear divergences and its UV divergence can only be attributed to mass renormalization. Further-

more it has IR singularities. The fermion-loop part only has UV divergences due to coupling-constant renormalization. Note that collinear singularities in the fermion-loop part, which can be traced back to the light quarks, have been regulated by giving each quark a mass m_f. The O and K part contain all types of singularities mentioned above.

The IR singularities cancel when one adds the virtual and soft contributions to the cross section. The latter will be presented in Sec. V. The UV singularities are removed by renormalization. Since the cross section is a renormalization-group invariant we can limit ourselves to mass and coupling-constant renormalization. Starting with the mass renormalization we have to choose the on-shell renormalization scheme in order to satisfy the Ward identity (3.1). This can be achieved by replacing the bare mass in the Born cross section by the renormalized mass:

$$m_b \to m\left[1+\frac{\alpha_s}{4\pi}C_F\left[\frac{6}{\epsilon}+3\gamma_E-3\ln 4\pi-4-3\ln\frac{\mu^2}{m^2}\right]\right]. \tag{3.7}$$

Here C_F denotes the Casimir factor which is determined by the representation of the fermion

$$C_F=\frac{N^2-1}{2N},\quad C_F=1,\quad C_F=N\ , \tag{3.8}$$

for (2.1), (2.3), and (2.4), respectively. $\alpha_s=g^2/4\pi$ is the strong coupling constant for (2.1), as well as (2.4). $\alpha_s=\alpha=1.0/137.0$ for (2.3). γ_E is Eulers constant. For the coupling-constant renormalization we have more freedom as long as we limit ourselves to gauge-invariant subtraction schemes. Here we will choose the modified minimal-subtraction ($\overline{\text{MS}}$) scheme with the mass of the heavy flavor m as renormalization scale. This will be achieved by replacing the bare coupling constant in the Born cross section by the renormalized one

$$g_b \to g\left[1+\frac{\alpha_s}{8\pi}\left[\frac{2}{\epsilon}+\gamma_E-\ln 4\pi-\ln\frac{\mu^2}{m^2}\right]\beta_0\right] \tag{3.9}$$

with α_s as before. β_0 denotes the lowest-order coefficient of the β function. It can be split into a gluon part β_g and a fermion part β_f:

$$\beta_0=\beta_{0,g}+\beta_{0,f}\ , \tag{3.10}$$

where β_g and β_f are determined by the representations of the gluon and the fermion with respect to their local and global gauge groups. In our example $\beta_{0,g}$ is given by

$$\beta_{0,g}=\tfrac{11}{3}N,\quad \beta_{0,g}=0,\quad \beta_{0,g}=\tfrac{11}{3}N\ , \tag{3.11}$$

for (2.1), (2.3), and (2.4), respectively, where we have assumed that the gluon is always a singlet with respect to the global gauge group. For $\beta_{0,f}$ we have

$$\beta_{0,f}=-\tfrac{2}{3}n_f,\quad \beta_{0,f}=-\tfrac{4}{3},\quad \beta_{0,f}=-\tfrac{2}{3}n_fN\ , \tag{3.12}$$

for (2.1), (2.3), and (2.4), respectively. In the case of (2.1) we have put the quark in the fundamental representation of the local, as well as the global gauge group. The dimension of the latter is indicated by n_f. The gluino in (2.4) is put in the adjoint representation of the local gauge group.

Other subtraction schemes and/or renormalization scales can be obtained via finite renormalizations. The renormalized virtual cross section is now given by

$$s^2\left[\frac{d^2\sigma_{gg}^{(1)}}{dt_1du_1}\right]_R^V=s^2\left[\frac{d^2\sigma_{gg}^{(1)}}{dt_1du_1}\right]^V+\frac{\alpha_s}{2\pi}\left[\frac{2}{\epsilon}+\gamma_E-\ln 4\pi-\ln\frac{\mu^2}{m^2}\right]\times\beta_0 s^2\frac{d^2\sigma_{gg}^{(0)}}{dt_1du_1}\ , \tag{3.13}$$

where mass renormalization in the first term of the right-hand side of the above equation is already implicitly understood.

IV. GLUON BREMSSTRAHLUNG

The gluon bremsstrahlung cross section is given by the process

$$g(k_1)+g(k_2)\to g(k_3)+Q(p_1)+\bar{Q}(p_2)\ . \tag{4.1}$$

This reaction is derived from the basic process in (2.1) by adding a gluon to the final state. Similar reactions exist for the processes in (2.3) and (2.4). The eleven Feynman diagrams which contribute to the amplitude $M^R_{\mu\nu\lambda}$ are shown in Fig. 4. In the calculation of these diagrams we

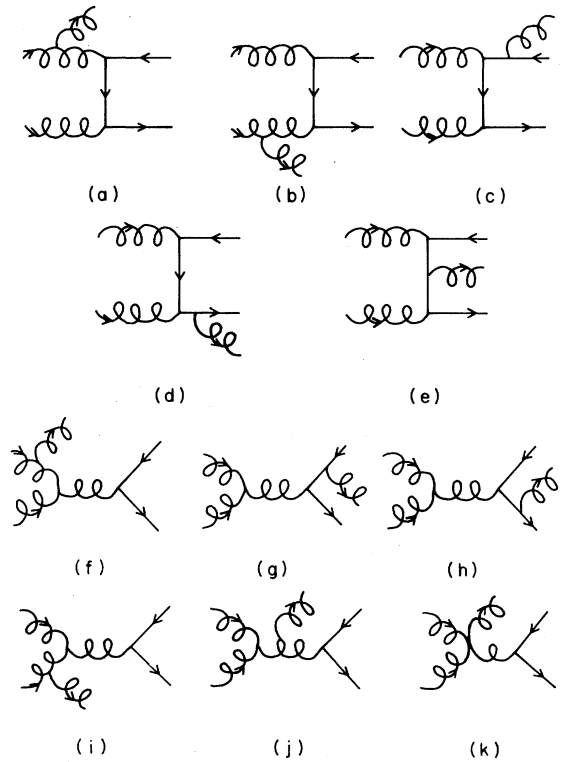

FIG. 4. The order-g^3 Feynman diagrams contributing to the amplitude for the gluon bremsstrahlung reaction $g(k_1)+g(k_2)\to Q(p_1)+\bar{Q}(p_2)+g(k_3)$. Additional graphs are obtained from (a)–(e) by reversing the arrows on the external lines.

found it convenient to introduce ten kinematical invariants:

$$\begin{aligned}
s &= (k_1+k_2)^2 , \\
s_3 &= (k_3+p_2)^2-m^2 , \\
s_4 &= (k_3+p_1)^2-m^2 , \\
s_5 &= (p_1+p_2)^2=-u_5 , \\
t_1 &= (k_2-p_2)^2-m^2=t-m^2 , \\
u_1 &= (k_1-p_2)^2-m^2=u-m^2 , \\
t' &= (k_2-k_3)^2 , \\
u' &= (k_1-k_3)^2 , \\
u_6 &= (k_2-p_1)^2-m^2 , \\
u_7 &= (k_1-p_1)^2-m^2 ,
\end{aligned} \tag{4.2}$$

where $k_1+k_2=k_3+p_1+p_2$. The invariants s, t_1, and u_1 were already used in the calculation of the Born graphs (Sec. II) and the virtual graphs (Sec. III). Since we are considering a two-to-three-body process only five of the invariants are linearly independent. The square of the amplitude summed over all spins and (physical) polarizations of the gluon is given by $\sum M^R M^{R*}$ where M^R is defined by

$$M^R=\epsilon^{\mu}(k_1)\epsilon^{\nu}(k_2)\epsilon^{\lambda}(k_3)M^R_{\mu\nu\lambda}(k_1,k_2,k_3) . \tag{4.3}$$

As in the case of the Born and virtual amplitude we only sum over the physical gluon polarizations. For this purpose we again use $P_l^{\mu\nu}$ in (2.9). The gauge invariance of the matrix element squared can be checked by the observation that the explicit dependence on n_l in (2.9) drops out. The square of the amplitude was calculated in n dimensions up to order ϵ^2 ($\epsilon=n-4$) in order to account for the IR and M singularities which show up in the real-gluon cross section. We checked algebraically that the $n=4$ part of the square of the matrix element agrees with the expressions already found in Ellis and Sexton[12] and Gunion and Kunszt.[17] Following the notation in the latter reference we write

$$\sum M^R M^{R*}=g^6(NC_O R_O+NC_K R_K+\bar{C}_{\rm QED}R_{\rm QED}) , \tag{4.4}$$

where C_O, C_K are defined in (2.8) and $\bar{C}_{\rm QED}$ is defined in (3.4) for the process in (2.1), (2.3), and (2.4), respectively.

Averaging over initial spins and colors the cross section can be written in the form (see Appendix B)

$$s^2\left[\frac{d^2\sigma^{(1)}_{gg}}{dt_1 du_1}\right]^R=\left[\frac{1}{2}\right]^3\frac{S_\epsilon^2\mu^{-\epsilon}}{\Gamma(1+\epsilon)}K\left[\frac{t_1u_1-sm^2}{\mu^2 s}\right]^{\epsilon/2}\times\frac{s_4^{1+\epsilon}}{(s_4+m^2)^{1+\epsilon/2}}\int d\Omega_n\sum M^R M^{R*} , \tag{4.5}$$

with $s_4=s+t_1+u_1$ and $d\Omega_n=\sin^{1+\epsilon}\theta_1 d\theta_1\sin^{\epsilon}\theta_2 d\theta_2$. Like the virtual and Born cross section we can decompose (4.5) into

$$(d\sigma^{(1)}_{gg})^R=(d\sigma^{(1)}_{gg,O})^R+(d\sigma^{(1)}_{gg,K})^R+(d\sigma^{(1)}_{gg,\rm QED})^R . \tag{4.6}$$

In order to perform the angular integrations the square of the matrix element has to be split into sets of terms of the type $(s')^k(s'')^l$. Here k,l are positive or negative integers and s',s'' represent pairs of the kinematical variables listed in (4.2). The decomposition has to be done in such a way that only one variable contains the polar angle θ_1 and the other one has both the polar angle θ_1 and the azimuthal angle θ_2. The decomposition requires extensive partial fractioning which exploits the following identities between the invariants defined in (4.2):

$$\begin{aligned}
s_3 &= u_5-t_1-u_1 , \\
s_4 &= u_5-u_6-u_7 , \\
u_5 &= -s-t'-u' , \\
u_6 &= -s-t_1-t' , \\
u_7 &= -s-u_1-u' .
\end{aligned} \tag{4.7}$$

Using these relations one can write each term in the square of the amplitude as a product of invariants, where the number of invariants containing the angular integration variables is two or less: e.g.,

$$t'^{-1}u'^{-1}u_5^{-1}=-s^{-1}(t'^{-1}u_5^{-1}+u'^{-1}u_5^{-1}+t'^{-1}u'^{-1}) . \tag{4.8}$$

We used SCHOONSCHIP to perform this decomposition. The resulting expression contains 80 distinct terms. After substituting the angles into the expressions for $(s')^k(s'')^l$ the result (4.5) requires the evaluation of integrals of the form

$$I_n^{(k,l)}=\int_0^{\pi}d\theta_1\sin^{n-3}\theta_1\times\int_0^{\pi}d\theta_2\sin^{n-4}\theta_2(a+b\cos\theta_1)^{-k}\times(A+B\cos\theta_1+C\sin\theta_1\cos\theta_2)^{-l} , \tag{4.9}$$

where a, b, A, B, and C are functions of the external kinematic variables s, t_1, u_1, and m^2. The results for the angular integrals are listed in Appendix C. Some of these integrals can be found in the literature[24–26] and the general method of evaluating them follows the techniques in Ref. 24.

Expression (4.9) contains collinear (M) singularities if $k\geq 1$ or $l\geq 1$ and $a^2=b^2$ or $A^2=B^2+C^2$ which arise when the outgoing gluon is emitted parallel to one of the incoming gluons. These singularities can be traced to the terms t'^{-1} and u'^{-1} in the square of the matrix element. The M singularities only show up in the O and K part of the cross section since the gluon is only emitted from a massive quark in the QED part. Besides the collinear divergences there are also IR singularities arising from soft-gluon emission. They show up when the cross section in (4.5) is convoluted with the input (bare) gluon distribution functions. The hadronic cross section (see also

Sec. VII) is defined by

$$S^2\frac{d^2\sigma^{H_1H_2}}{dT_1dU_1}=\int_{x_{1-}}^1\frac{dx_1}{x_1}\int_{x_{2-}}^1\frac{dx_2}{x_2}f_g^{H_1}(x_1)f_g^{H_2}(x_2)\times s^2\frac{d^2\sigma_{gg}}{dt_1du_1}\ , \tag{4.10}$$

where S, T_1, and U_1 (see Sec. VII) are the hadronic analogues of the parton kinematic variables s, t_1, and u_1 defined in (2.2). f_g^H denotes the bare parton (bare gluon) distribution function whereas $d^2\sigma_{gg}$ stands for the various parton cross sections (Born, virtual and real gluon) calculated in this paper. The limits x_{1-} and x_{2-} are determined by the kinematical conditions

$$\begin{aligned}&s=x_1x_2S,\quad t_1=x_1T_1\ ,\\&u_1=x_2U_1\quad\text{with } 0\le x_1\le 1,\ 0\le x_2\le 1\ ,\\&s_4=x_1x_2S+x_1T_1+x_2U_1\ge 0\ ,\end{aligned} \tag{4.11}$$

which yield

$$x_{1-}=\frac{-U_1}{S+T_1},\quad x_{2-}=\frac{-x_1T_1}{x_1S+U_1}\ . \tag{4.12}$$

For a plot of the kinematics, see Fig. 5. If the real-gluon cross section in (4.5) is inserted into (4.10) we get IR singularities which arise at the end point of the integration $x_2=x_{2-}$. At this point $s_4=0$ and the gluon momentum k_3 vanishes. To study this phenomenon further we make a change of variable in (4.10) via $x_2=(s_4-x_1T_1)/(x_1S+U_1)$ and integrate over s_4 rather than x_2. Then we split the integral over s_4 as follows:

$$\begin{aligned}S^2\frac{d^2\sigma^{H_1H_2}}{dT_1dU_1}=\int_{x_{1-}}^1\frac{dx_1}{x_1}\frac{1}{s_4-x_1T_1}&\times\left[\int_\Delta^{x_1(S+T_1)+U_1}ds_4+\int_0^\Delta ds_4\right]\\&\times f_g^{H_1}(x_1)f_g^{H_2}\left[\frac{s_4-x_1T_1}{x_1S+U_1}\right]\\&\times\left[s^2\frac{d^2\sigma_{gg}}{dt_1du_1}\right]^R.\end{aligned} \tag{4.13}$$

If we now choose $\Delta\ll m^2,S,T_1,U_1$, which implies $\Delta\ll s,t_1,u_1$, then one can approximate the second integral in (4.13) by

$$\int_{x_{1-}}^1\frac{dx_1}{x_1}\frac{-1}{x_1T_1}f_g^{H_1}(x_1)f_g^{H_2}\left[\frac{-x_1T_1}{x_1S+U_1}\right]\times\int_0^\Delta ds_4\left[s^2\frac{d^2\sigma_{gg}}{dt_1du_1}\right]^R. \tag{4.14}$$

Note that in this approximation one neglects terms of the order Δ/m^2, Δ/S, Δ/T_1, and Δ/U_1. This will not cause problems since Δ will be set to zero in the final answer (see Secs. VI and VII). The result (4.14) is just a convolution integral of the type in (4.10) over a δ function which appears in the case of the Born and virtual cross sections. Since $0\le s_4\le\Delta$ represents the soft-gluon region we can define the soft-gluon cross section as

$$\left[s^2\frac{d^2\sigma_{gg}^{(1)}}{dt_1du_1}\right]^S=\delta(s+t_1+u_1)\int_0^\Delta ds_4\left[s^2\frac{d^2\sigma_{gg}^{(1)}}{dt_1du_1}\right]^R. \tag{4.15}$$

Insertion of expression (4.15) into (4.10) leads immediately to (4.14). The above cross section contains all IR singularities. The double-pole terms are those containing the factors $t'^{-1}u'^{-1},t'^{-1}s_3^{-1},u'^{-1}s_3^{-1},t'^{-1}s_4^{-1},u'^{-1}s_4^{-1}$, whereas the single-pole terms contain the factors s_3^{-2}, s_4^{-2} and $s_3^{-1}s_4^{-1}$. The last set of terms, which lead to IR divergences, only show up in the QED part. The O and K part of the matrix element contains both sets of terms. The first will be often referred to as the soft-collinear term.

The part of the matrix element contributing to the soft-gluon integral in (4.15) can be obtained via the eikonal approximation. Here one neglects the soft-gluon momenta on the quark lines with respect to the quark momenta. However the three gluon vertices have to be treated exactly. Notice that this method also applies to the kinematics so that the gluon momentum which appears in the overall momentum-conserving δ function in (B8) can be neglected with respect to the other momenta. In this way the 2-3 particle kinematics becomes equivalent to the kinematics in a 2-2 particle reaction so one immediately obtains the δ function in (4.15). This method provides us with the soft-gluon matrix element, which has to be computed up to order ϵ^2 in order to account for the soft-collinear divergences. From this result we infer the soft-gluon cross section which will be presented in the next section. If one adds the renormalized virtual cross section (3.13) to the soft-gluon cross section (4.15) the IR divergences cancel. This implies that all double poles cancel and the ones left over are only due to collinear singularities. They will eventually be removed by mass factorization (Sec. VI).

The other piece of the s_4 integration, which ranges from $\Delta<s_4<x_1(S+T_1)+U_1$, yields the hard-gluon cross section. The hard-gluon matrix element squared has to be computed up to order ϵ as far as the terms t'^{-1} and u'^{-1} are concerned. As has been already mentioned below (4.9) these terms represent the hard collinear (M) divergences which can be removed by mass factorization. According to (4.6) the hard-gluon cross section contains the pieces

$$s^2\left[\frac{d^2\sigma_{gg,O}^{(1)}}{dt_1du_1}\right]^H=\tfrac{1}{4}\alpha_s^3KNC_O\left[\frac{t_1u_1-sm^2}{\mu^2s}\right]^{\epsilon/2}\times\left\{\left\{\left[\frac{(s+t_1)^2+u_1^2}{(s+t_1)(s+t_1+u_1)}-\frac{(s+t_1)^2+(s+t_1+u_1)^2}{(s+t_1)u_1}-\frac{u_1^2+(s+t_1+u_1)^2}{(s+t_1)^2}\right]\right.\right.$$

$$\times\left[\frac{t_1^2+(s+t_1)^2}{t_1u_1}\left[\frac{t_1^2+(s+t_1)^2}{s^2(s+t_1)}-\frac{4m^2}{su_1}+\frac{4m^4}{t_1u_1^2}\right]\left[\frac{2}{\epsilon}+\gamma_E-\ln4\pi+\ln\frac{(s+t_1+u_1)^2}{\mu^2(s+t_1+u_1+m^2)}\right]\right.$$
$$\left.+2\left[\frac{(s+t_1)^2}{u_1s^2}+\frac{t_1^2}{u_1s^2}+\frac{s+t_1}{t_1u_1}+\frac{t_1}{u_1(s+t_1)}\right]\right]$$
$$+\frac{4m^2(s+t_1+u_1)}{u_1^2}\left[\frac{t_1^2+(s+t_1)^2}{st_1u_1}-\frac{m^2[t_1^2+(s+t_1)^2]}{t_1^2u_1^2}\right]\Bigg\}+\{t_1\leftrightarrow u_1\}\Bigg]$$
$$+\left[\frac{1}{2}\right]^5\frac{\alpha_s^3}{\pi}KNC_O\frac{s+t_1+u_1}{s+t_1+u_1+m^2}\left[\int d\Omega_n R_O\right]^{\text{finite}}, \tag{4.16}$$

$$s^2\left[\frac{d^2\sigma_{gg,K}^{(1)}}{dt_1du_1}\right]^H=-\tfrac{1}{4}\alpha_s^3KNC_K\left[\frac{t_1u_1-sm^2}{\mu^2s}\right]^{\epsilon/2}$$
$$\times\left[\left\{\left[\frac{(s+t_1)^2+u_1^2}{(s+t_1)(s+t_1+u_1)}-\frac{(s+t_1)^2+(s+t_1+u_1)^2}{(s+t_1)u_1}-\frac{u_1^2+(s+t_1+u_1)^2}{(s+t_1)^2}\right]\right.\right.$$
$$\times\left[\left[\frac{t_1^2+(s+t_1)^2}{t_1u_1(s+t_1)}-\frac{4m^2s}{t_1u_1^2}+\frac{4m^4s^2}{t_1^2u_1^3}\right]\left[\frac{2}{\epsilon}+\gamma_E-\ln4\pi+\ln\frac{(s+t_1+u_1)^2}{\mu^2(s+t_1+u_1+m^2)}\right]\right.$$
$$\left.\left.+2\left[\frac{1}{u_1}+\frac{s^2}{t_1u_1(s+t_1)}\right]\right]+\frac{4m^2s(s+t_1+u_1)}{t_1u_1^2}\left[\frac{1}{u_1}-\frac{m^2s}{t_1u_1^2}\right]\Bigg\}+\{t_1\leftrightarrow u_1\}\Bigg]$$
$$-\left[\frac{1}{2}\right]^5\frac{\alpha_s^3}{\pi}KNC_K\frac{s+t_1+u_1}{s+t_1+u_1+m^2}\left[\int d\Omega_n R_K\right]^{\text{finite}}, \tag{4.17}$$

and

$$s^2\left[\frac{d^2\sigma_{gg,\text{QED}}^{(1)}}{dt_1du_1}\right]^H=\left[\frac{1}{2}\right]^5\frac{\alpha_s^3}{\pi}K\bar{C}_{\text{QED}}\frac{s+t_1+u_1}{s+t_1+u_1+m^2}\int d\Omega_4 R_{\text{QED}}, \tag{4.18}$$

where the symbol $(\ )^{\text{finite}}$ denotes the finite part of the angular integrals listed in Appendix C. The expressions for the squares of the matrix elements, namely, R_O, R_K, and R_{QED}, can now be taken in four dimensions. Because of the notational differences, they are 8 times smaller than their namesakes in Table I of Ref. 17.

V. SOFT-GLUON CORRECTIONS

The soft-gluon amplitude can be obtained from the matrix element in (4.3) by applying the eikonal approximation. The limit $k_3\to0$ is taken in the numerator and denominator terms as has been indicated in the previous section [see the text below (4.15)]. In this limit the kinematical invariants in the two-to-three-body process can be approximated by

$$s_3\to0,\quad s_4\to0,\quad t'\to0,\quad u'\to0,\quad u_5\to-s,\quad u_6\to u_1,\quad u_7\to t_1, \tag{5.1}$$

while the other invariants remain unaltered. The soft matrix element can be written in the following form [see (4.4)]:

$$\sum M^S M^{S*}=g^6(NC_OS_O+NC_KS_K+\bar{C}_{\text{QED}}S_{\text{QED}}), \tag{5.2}$$

with

$$S_O=4\left[\frac{t_1u_1^2}{s^2}\left[\frac{1}{u's_4}+\frac{1}{t's_3}\right]+\frac{t_1^2u_1}{s^2}\left[\frac{1}{t's_4}+\frac{1}{u's_3}\right]+\frac{t_1^2+u_1^2}{s^2}\left[\frac{s}{t'u'}-\frac{m^2}{s_3^2}-\frac{m^2}{s_4^2}\right]\right]B_{\text{QED}}, \tag{5.3}$$

$$S_K=4\left[-t_1\left[\frac{1}{u's_4}+\frac{1}{t's_3}\right]-u_1\left[\frac{1}{t's_4}+\frac{1}{u's_3}\right]+\left[2+\frac{t_1^2+u_1^2}{s^2}\right]\left[\frac{m^2}{s_3^2}+\frac{m^2}{s_4^2}\right]-\frac{t_1^2+u_1^2}{s^2}\frac{s-2m^2}{s_3s_4}\right]B_{\text{QED}}, \tag{5.4}$$

and

$$S_{\text{QED}}=-4\left[\frac{m^2}{s_3^2}+\frac{m^2}{s_4^2}-\frac{s-2m^2}{s_3s_4}\right]B_{\text{QED}}, \tag{5.5}$$

where B_{QED} is given in (2.7). From (4.5) and (4.15) we infer the soft-gluon cross section

$$s^2\left[\frac{d^2\sigma_{gg}^{(1)}}{dt_1du_1}\right]^S=\left[\frac{1}{2}\right]^3\frac{S_\epsilon^2\mu^{-\epsilon}}{\Gamma(1+\epsilon)}K\left[\frac{t_1u_1-sm^2}{\mu^2 s}\right]^{\epsilon/2}\delta(s+t_1+u_1)\int_0^\Delta ds_4\frac{s_4^{1+\epsilon}}{(s_4+m^2)^{1+\epsilon/2}}\int d\Omega_n\sum M^S M^{S*}\ . \tag{5.6}$$

Using the expressions for the angular integrals in Appendix C the integration over s_4 is straightforward. Decomposing the soft cross section as indicated in (5.2) we obtain

$$\begin{aligned}s^2\left[\frac{d^2\sigma_{gg,O}^{(1)}}{dt_1du_1}\right]^S&=KNC_O F(s,t_1,u_1)\delta(s+t_1+u_1)\\&\times\left\{\frac{t_1^2+u_1^2}{s^2}\left[-\frac{s-2m^2}{\sqrt{s^2-4sm^2}}\ln x-\frac{2}{\epsilon}+1+\frac{8}{\epsilon^2}+\frac{2}{\epsilon}\ln\frac{sm^2}{t_1u_1}\right.\right.\\&\qquad\left.+\tfrac{1}{2}\ln^2\frac{sm^2}{t_1u_1}-\ln^2 x+\mathrm{Li}_2\left[1-\frac{sm^2}{t_1u_1}\right]-3\zeta(2)\right]\\&+\frac{t_1^2}{s^2}\left[\frac{2}{\epsilon}\ln\frac{u_1}{t_1}+\frac{1}{2}\ln^2\frac{xt_1}{u_1}+\mathrm{Li}_2\left[1-\frac{u_1}{xt_1}\right]-\mathrm{Li}_2\left[1-\frac{t_1}{xu_1}\right]\right]\\&\left.+\frac{u_1^2}{s^2}\left[\frac{2}{\epsilon}\ln\frac{t_1}{u_1}+\frac{1}{2}\ln^2\frac{xu_1}{t_1}+\mathrm{Li}_2\left[1-\frac{t_1}{xu_1}\right]-\mathrm{Li}_2\left[1-\frac{u_1}{xt_1}\right]\right]\right\},\end{aligned} \tag{5.7}$$

$$\begin{aligned}s^2\left[\frac{d^2\sigma_{gg,K}^{(1)}}{dt_1du_1}\right]^S&=KNC_K F(s,t_1,u_1)\delta(s+t_1+u_1)\\&\times\left[-\frac{8}{\epsilon^2}+\ln^2 x-\ln^2\frac{u_1}{t_1}+3\zeta(2)+\left[2+\frac{t_1^2+u_1^2}{s^2}\right]\left[\frac{s-2m^2}{\sqrt{s^2-4sm^2}}\ln x+\frac{2}{\epsilon}-1\right]\right.\\&\left.-\frac{t_1^2+u_1^2}{s^2}\frac{s-2m^2}{\sqrt{s^2-4sm^2}}\left[-\frac{2}{\epsilon}\ln x+2\,\mathrm{Li}_2(x)+2\,\mathrm{Li}_2(-x)-\ln^2 x+2\ln x\ln(1-x^2)-\zeta(2)\right]\right],\end{aligned} \tag{5.8}$$

$$\begin{aligned}s^2\left[\frac{d^2\sigma_{gg,\mathrm{QED}}^{(1)}}{dt_1du_1}\right]^S&=K\bar{C}_{\mathrm{QED}}F(s,t_1,u_1)\delta(s+t_1+u_1)\\&\times\left\{\frac{s-2m^2}{\sqrt{s^2-4sm^2}}\left[-\left[\frac{2}{\epsilon}+1\right]\ln x+2\,\mathrm{Li}_2(x)+2\,\mathrm{Li}_2(-x)-\ln^2 x+2\ln x\ln(1-x^2)-\zeta(2)\right]-\frac{2}{\epsilon}+1\right\},\end{aligned} \tag{5.9}$$

with

$$x=\frac{1-\sqrt{1-4m^2/s}}{1+\sqrt{1-4m^2/s}},\quad 0\le x\le 1\ , \tag{5.10}$$

and the common factor F defined by

$$\begin{aligned}F(s,t_1,u_1)&=\frac{1}{16\pi}g^6\frac{S_\epsilon}{\Gamma(1+\epsilon/2)}e^{\epsilon/2(\gamma_E-\ln 4\pi)}\\&\times\left[\frac{t_1u_1-sm^2}{\mu^2 s}\right]^{\epsilon/2}\left[\frac{\Delta^2}{\mu^2 m^2}\right]^{\epsilon/2}B_{\mathrm{QED}}\ .\end{aligned} \tag{5.11}$$

In the above expressions $\zeta(2)=\pi^2/6$ and γ_E is the Euler constant. $\mathrm{Li}_2(x)$ is the dilogarithmic function as defined in Ref. 27. Note that all differential cross sections are proportional to the QED part of the Born cross section. However, because of the typical non-Abelian character of this process the soft-gluon expression (5.6) is *not* proportional to the whole Born cross section [see (2.11)]. This is revealed by the fact that in the case of process (2.1) $\bar{C}_{\mathrm{QED}}=0$ whereas the $O(\alpha_s)$ part of the (5.6) yields $\bar{C}_{\mathrm{QED}}=(N^4-1)/N^2$ cf. (3.4). Addition of the renormalized virtual contribution (3.13) and the soft contribution (5.6) leads to the cancellation of the infrared singularities present in both of them. The leftover collinear singularities from the initial-state gluon radiation are responsible for the single-pole terms. The latter can be removed via mass factorization as will be shown in the next section.

VI. MASS FACTORIZATION

As has been mentioned in the previous sections the renormalized virtual plus soft- and hard-gluon cross sections still contain initial-state collinear divergences. These divergences have to be removed via mass factorization. The collinear-singular parton cross section $d\sigma_{ij}$ can be written to all orders in α_s as

$$s^2\frac{d^2\sigma_{ij}(s,t_1,u_1,\mu^2,\epsilon)}{dt_1du_1}$$
$$=\int_0^1\frac{dx_1}{x_1}\int_0^1\frac{dx_2}{x_2}\Gamma_{li}(x_1,Q^2,\mu^2,\epsilon)\Gamma_{mj}(x_2,Q^2,\mu^2,\epsilon)$$
$$\times\hat{s}^2\frac{d^2\hat{\sigma}_{lm}(\hat{s},\hat{t}_1,\hat{u}_1,Q^2)}{d\hat{t}_1d\hat{u}_1}\ , \tag{6.1}$$

where $\hat{s}=x_1x_2s$, $\hat{t}_1=x_1t_1$, $\hat{u}_1=x_2u_1$. The Γ_{li} are the splitting functions which have been calculated up to order α_s^2 and can be found in the literature.[28] They contain singularities as poles in ϵ and further depend on the mass factorization scale Q^2, which is of the order of s,t_1,u_1. The parameter μ^2 is an artifact of n-dimensional regularization which appears in the splitting function as well as in the parton cross section $d\sigma_{ij}$. The reduced cross section $d\hat{\sigma}_{lm}$ has no collinear divergences and is therefore finite in the limit $\epsilon\to0$. The above equation holds for the nonsinglet as well as singlet case. Like the Γ_{ij}, the parton cross sections $d\hat{\sigma}_{lm}$ can be expanded in a power series in α_s as follows:

$$s^2\frac{d^2\sigma_{ij}}{dt_1du_1}=\sum_{n=0}^{\infty}s^2\frac{d^2\sigma_{ij}^{(n)}}{dt_1du_1}\ ,$$
$$\hat{s}^2\frac{d^2\hat{\sigma}_{lm}}{dt_1du_1}=\sum_{n=0}^{\infty}\hat{s}^2\frac{d^2\hat{\sigma}_{lm}^{(2)}}{dt_1du_1}\ . \tag{6.2}$$

Here $d\sigma_{ij}^{(n)}$ and $d\hat{\sigma}_{lm}^{(n)}$ represent the order-α_s^n part of the collinear-singular and collinear-finite cross sections. In this section we will calculate the reduced cross section $d\hat{\sigma}_{gg}^{(1)}$ which is obtained from $d\sigma_{gg}^{(1)}$. The latter receives its contribution from the hard-gluon cross section (4.16)–(4.18) and the virtual plus soft parts in (3.13) and (5.7)–(5.11). The gluon-gluon splitting function Γ_{gg} has been calculated in the literature.[28] Up to order α_s it can be written as

$$\Gamma_{gg}(x_i,Q^2,\mu^2,\epsilon)=\delta(1-x_i)+\frac{\alpha_s}{2\pi}\left[P_{gg}(x_i,\delta_i)\frac{2}{\epsilon}+\sum_{f=L}P_{gg}^f(x_i)\ln\frac{m_f^2}{m^2}+f_{gg}(x_i,Q^2,\mu^2,\delta_i)\right]\ , \tag{6.3}$$

where the sum is over the light flavors $L=(u,d,s)$. As has been mentioned above (3.1) the collinear divergences due to the light quarks have been regulated by giving these quarks a small mass m_f. This implies that the collinear pole term ϵ^{-1} is replaced by the logarithmic singular term $\ln m_f^2/m^2$. The gluon contribution P_{gg} and the fermion-loop contribution P_{gg}^f are given by

$$P_{gg}(x_i,\delta_i)=N\left[\theta(1-x_i-\delta_i)\times\left[\frac{2}{1-x_i}+\frac{2}{x_i}-4+2x_i-2x_i^2\right]+\delta(1-x_i)(2\ln\delta_i+\tfrac{11}{6})\right]\ , \tag{6.4}$$

$$P_{gg}^f(x_i)=\delta(1-x_i)(-\tfrac{1}{2}\tilde{\beta}_{0,f})\ . \tag{6.5}$$

where $\tilde{\beta}_{0,f}$ is obtained from β_0, in (3.12) by putting $n_f=1$.

The function $f_{gg}(x_i,Q^2,\mu^2,\delta_i)$ does not contain collinear divergences and can be chosen arbitrarily. This implies that the reduced cross section $d\hat{\sigma}$ depends on the way one has performed the mass factorization in (6.1). This is indicated by the mass factorization scale Q^2 which appears in $d\hat{\sigma}$ as well as in f_{gg} and Γ_{gg}. In order to regulate the pole at $x_i=1$, which appears in Γ_{gg} as well as in f_{gg} we have adopted the convention in Ref. 29. Here one introduces a parameter δ_i which enables us to distinguish between soft gluons, where $x_i>1-\delta_i$ and hard gluons where $x_i<1-\delta_i$. The parameter δ_i is related to the quantity Δ which appears in the soft-gluon factor in (5.11) via mass factorization. Substituting (6.2) into (6.1) we obtain the following relations between the coefficients $d\sigma_{ij}^{(n)}$ and $d\hat{\sigma}_{lm}^{(n)}$:

$$s^2\frac{d^2\hat{\sigma}_{gg}^{(0)}(s,t_1,u_1)}{dt_1du_1}=s^2\frac{d^2\sigma_{gg}^{(0)}(s,t_1,u_1)}{dt_1du_1} \tag{6.6}$$

and

$$s^2\frac{d^2\hat{\sigma}_{gg}^{(1)}(s,t_1,u_1)}{dt_1du_1}=s^2\frac{d^2\sigma_{gg}^{(1)}(s,t_1,u_1)}{dt_1du_1}$$
$$-\frac{\alpha_s}{2\pi}\left[\int_0^1\frac{dx_1}{x_1}\left[P_{gg}(x_1,\delta_1)\frac{2}{\epsilon}+\sum_{f=L}P_{gg}^f(x_1)\ln\frac{m_f^2}{m^2}+f_{gg}(x_1,Q^2,\mu^2,\delta_1)\right]\hat{s}^2\frac{d^2\hat{\sigma}_{gg}^{(0)}(x_1s,x_1t_1,u_1)}{d\hat{t}_1du_1}\right.$$
$$+\int_0^1\frac{dx_2}{x_2}\left[P_{gg}(x_2,\delta_2)\frac{2}{\epsilon}+\sum_{f=L}P_{gg}^f(x_2)\ln\frac{m_f^2}{m^2}+f_{gg}(x_2,Q^2,\mu^2,\delta_2)\right]$$
$$\left.\times\hat{s}^2\frac{d^2\hat{\sigma}_{gg}^{(0)}(x_2s,t_1,x_2u_1)}{dt_1d\hat{u}_1}\right]\ . \tag{6.7}$$

Notice that we have used the relation (6.6) in deriving (6.7). From (6.3)–(6.5) we infer that P_{gg} and f_{gg} can be split into two pieces as follows:

$$P_{gg}(x_i,\delta_i)=\theta(1-x_i-\delta_i)P_{gg}^{H}(x_i)+\delta(1-x_i)P_{gg}^{S+V}(\delta_i)\ ,$$
$$f_{gg}(x_i,Q^2,\mu^2,\delta_i)=\theta(1-x_i-\delta_i)f_{gg}^{H}(x_i,Q^2,\mu^2)+\delta(1-x_i)f_{gg}^{S+V}(Q^2,\mu^2,\delta_i)\ , \tag{6.8}$$

where P^H,f^H and P^{S+V},f^{S+V} denote the hard- and soft-gluon parts, respectively. Substitution of (6.6) and (6.8) into (6.7) yields

$$\begin{aligned}s^2\frac{d^2\hat{\sigma}_{gg}^{(1)}(s,t_1,u_1)}{dt_1du_1}=&s^2\frac{d^2\sigma_{gg}^{(1)}(s,t_1,u_1)}{dt_1du_1}\\&-\frac{\alpha_s}{2\pi}\left[[P_{gg}^{S+V}(\delta_1)+P_{gg}^{S+V}(\delta_2)]\frac{2}{\epsilon}-\sum_{f=L}\tilde{\beta}_{0,f}\ln\frac{m_f^2}{m^2}+f_{gg}^{S+V}(Q^2,\mu^2,\delta_1)+f_{gg}^{S+V}(Q^2,\mu^2,\delta_2)\right]\\&\times s^2\frac{d^2\sigma_{gg}^{(0)}(s,t_1,u_1)}{dt_1du_1}\\&-\frac{\alpha_s}{2\pi}\left[\int_0^{1-\delta_1}\frac{dx_1}{x_1}\left[P_{gg}^{H}(x_1)\frac{2}{\epsilon}+f_{gg}^{H}(x_1,Q^2,\mu^2)\right]\hat{s}^2\frac{d^2\sigma_{gg}^{(0)}(x_1s,x_1t_1,u_1)}{d\hat{t}_1du_1}\right.\\&\left.+\int_0^{1-\delta_2}\frac{dx_2}{x_2}\left[P_{gg}^{H}(x_2)\frac{2}{\epsilon}+f_{gg}^{H}(x_2,Q^2,\mu^2)\right]\hat{s}^2\frac{d^2\sigma_{gg}^{(0)}(x_2s,t_1,x_2u_1)}{dt_1d\hat{u}_1}\right]\ .\end{aligned} \tag{6.9}$$

From the $\delta(s+t_1+u_1)$ factor in the Born cross section for $d^2\sigma_{gg}^{(0)}$ in (2.14) we infer that the first and second integrals between the large square brackets of (6.9) are evaluated for

$$x_1=\frac{-u_1}{s+t_1},\quad x_2=\frac{-t_1}{s+u_1}\ , \tag{6.10}$$

respectively, with the constraints $x_1<1-\delta_1$ and $x_2<1-\delta_2$. This implies that

$$\delta_1<1+\frac{u_1}{s+t_1},\quad \delta_2<1+\frac{t_1}{s+u_1}\ . \tag{6.11}$$

From he soft-gluon integral in (5.6) we observe that the kinematical invariants s,t_1,u_1 in the hard-gluon part of $d^2\sigma_{gg}^{(1)}$ in (6.9) satisfy the inequality (see also Sec. IV)

$$s_4=s+t_1+u_1>\Delta\ . \tag{6.12}$$

From (6.11) and (6.12) it follows that we can identify

$$\delta_1=\frac{\Delta}{s+t_1},\quad \delta_2=\frac{\Delta}{s+u_1}\ . \tag{6.13}$$

As has already been pointed out in the text after (6.5), $d\hat{\sigma}_{gg}^{(1)}$ depends on the choice we make for the function f_{gg}. Besides the dependency of the reduced cross section on coupling-constant renormalization as mentioned below (3.7), this now introduces a second arbitrariness. However, from a phenomenological viewpoint the latter is much more serious than the former. It is possible to find a process where the running coupling constant can be measured with a reasonable accuracy for a given renormalization scheme. Examples are the thrust distribution in $e^+e^-\rightarrow$hadrons and the nonsinglet structure function in deep-inelastic scattering. However, this is not the case for the gluon distribution function. Neither in deep-inelastic scattering nor in direct photon production ($g+q\rightarrow g+q+\gamma$) (Ref. 30) can we measure the gluon distribution function for a given mass-factorization prescription with a reasonable accuracy.

This is especially true for the large-x region. Here x stands for the fraction of the momentum of the hadron carried away by the gluon. This will seriously affect the predictive power of our calculation. Since we cannot do any better we have chosen the $\overline{\text{MS}}$ mass factorization scheme with $Q^2=m^2$ as factorization scale. This is the same scheme which was chosen for the coupling-constant renormalization. With this choice we have

$$f_{gg}(x_i,Q^2,\mu^2,\delta_i)=P_{gg}(x_i,\delta_i)\left[\gamma_E-\ln4\pi+\ln\frac{m^2}{\mu^2}\right]\ . \tag{6.14}$$

Other mass factorization schemes are also possible: see, e.g., Ref. 13.

The reduced cross section $d\hat{\sigma}_{gg}^{(1)}$ can now be split in the same way as has been done for the hard part in (4.6) and the virtual part in (3.6) so the hard-gluon part of the reduced cross section becomes

$$(d\hat{\sigma}_{gg}^{(1)})^H=(d\hat{\sigma}_{gg,O}^{(1)})^H+(d\hat{\sigma}_{gg,K}^{(1)})^H+(d\hat{\sigma}_{gg,\text{QED}}^{(1)})^H\ , \tag{6.15}$$

where the terms on the right-hand side of (6.15) are given by

$$s^2\left[\frac{d^2\hat{\sigma}^{(1)}_{gg,O}}{dt_1du_1}\right]^H=\tfrac{1}{4}\alpha_s^3 KNC_O\left[\frac{t_1^2+(s+t_1)^2}{st_1u_1}\left\{\left[\frac{(s+t_1)^2+u_1^2}{(s+t_1)(s+t_1+u_1)}-\frac{(s+t_1)^2+(s+t_1+u_1)^2}{(s+t_1)u_1}-\frac{u_1^2+(s+t_1+u_1)^2}{(s+t_1)^2}\right]\right.\right.$$
$$\times\left[\frac{t_1^2+(s+t_1)^2}{s(s+t_1)}-\frac{4m^2}{u_1}\left[1-\frac{sm^2}{t_1u_1}\right]\right]\ln\frac{(s+t_1+u_1)^2}{m^2(s+t_1+u_1+m^2)}$$
$$\left.\left.+\frac{8m^2(s+t_1+u_1)}{u_1^2}\left[1-\frac{sm^2}{t_1u_1}\right]\right\}+\{t_1\leftrightarrow u_1\}\right]$$
$$+\left[\frac{1}{2}\right]^5\frac{\alpha_s^3}{\pi}KNC_O\frac{s+t_1+u_1}{s+t_1+u_1+m^2}\left[\int d\Omega_n R_O\right]^{\text{finite}}, \tag{6.16}$$

$$s^2\left[\frac{d^2\hat{\sigma}^{(1)}_{gg,K}}{dt_1du_1}\right]^H=-\tfrac{1}{4}\alpha_s^3 KNC_K\left[\frac{s}{t_1u_1}\left\{\left[\frac{(s+t_1)^2+u_1^2}{(s+t_1)(s+t_1+u_1)}-\frac{(s+t_1)^2+(s+t_1+u_1)^2}{(s+t_1)u_1}-\frac{u_1^2+(s+t_1+u_1)^2}{(s+t_1)^2}\right]\right.\right.$$
$$\times\left[\frac{t_1^2+(s+t_1)^2}{s(s+t_1)}-\frac{4m^2}{u_1}\left[1-\frac{sm^2}{t_1u_1}\right]\right]\ln\frac{(s+t_1+u_1)^2}{m^2(s+t_1+u_1+m^2)}$$
$$\left.\left.+\frac{8m^2(s+t_1+u_1)}{u_1^2}\left[1-\frac{sm^2}{t_1u_1}\right]\right\}+\{t_1\leftrightarrow u_1\}\right]$$
$$+\left[\frac{1}{2}\right]^5\frac{\alpha_s^3}{\pi}KNC_K\frac{s+t_1+u_1}{s+t_1+u_1+m^2}\left[\int d\Omega_n R_K\right]^{\text{finite}}, \tag{6.17}$$

$$s^2\left[\frac{d^2\hat{\sigma}^{(1)}_{gg,\text{QED}}}{dt_1du_1}\right]^H=\left[\frac{1}{2}\right]^5\frac{\alpha_s^3}{\pi}K\bar{C}_{\text{QED}}\frac{s+t_1+u_1}{s+t_1+u_1+m^2}\int d\Omega_4 R_{\text{QED}}\ . \tag{6.18}$$

For the definitions of $(\ )^{\text{finite}}$ see the text below (4.18). The virtual- plus soft-gluon part of the reduced cross section can be written as [see (3.6)]

$$(d\hat{\sigma}^{(1)}_{gg})^{V+S}=(d\hat{\sigma}^{(1)}_{gg,O})^{V+S}+(d\hat{\sigma}^{(1)}_{gg,K})^{V+S}$$
$$+(d\hat{\sigma}^{(1)}_{gg,\text{QED}})^{V+S}+(d\hat{\sigma}^{(1)}_{gg,f})^{V+S}\ . \tag{6.19}$$

We are able to give an explicit expression for the right-hand side of (6.19). The first three terms are

$$s^2\left[\frac{d^2\hat{\sigma}^{(1)}_{gg,O}}{dt_1du_1}\right]^{V+S}=\tfrac{1}{16}\alpha_s^3 KNC_O[F_O^{V+S}(t,u,t_1,u_1)$$
$$+F_O^{V+S}(u,t,u_1,t_1)]\times\delta(s+t_1+u_1)\ ,$$
$$s^2\left[\frac{d^2\hat{\sigma}^{(1)}_{gg,K}}{dt_1du_1}\right]^{V+S}=\tfrac{1}{16}\alpha_s^3 KNC_K[F_K^{V+S}(t,u,t_1,u_1)$$
$$+F_K^{V+S}(u,t,u_1,t_1)]\times\delta(s+t_1+u_1)\ , \tag{6.20}$$
$$s^2\left[\frac{d^2\hat{\sigma}^{(1)}_{gg,\text{QED}}}{dt_1du_1}\right]^{V+S}=\tfrac{1}{16}\alpha_s^3 K\bar{C}_{\text{QED}}[F_{\text{QED}}^{V+S}(t,u,t_1,u_1)$$
$$+F_{\text{QED}}^{V+S}(u,t,u_1,t_1)]\times\delta(s+t_1+u_1)\ ,$$

where

$$F_O^{V+S}(t,u,t_1,u_1),\quad F_K^{V+S}(t,u,t_1,u_1)\ ,$$

and

$$F_{\text{QED}}^{V+S}(t,u,t_1,u_1)$$

can be found in Appendix D.

Notice that the apparent singularity at the threshold $s=4m^2$ (i.e., $s_1=0$), which is caused by terms containing s_1^{-2}, s_1^{-1} explicitly disappears from the expressions in F_K^{V+S} and F_{QED}^{V+S}. These pole terms are still present in F_O^{V+S}. However, one can check that for $s\to 4m^2$ the expressions in (D2) and (D3) behave like $\pi^2\bar{s}^{-1}$ where $\bar{s}=s\sqrt{1-4m^2/s}$; see (7.17). In the total cross section the last term will be canceled by the factor of $\bar{s}$ coming from the integration over phase space. This implies that the contribution of the virtual plus soft correction term in (6.20) leads to a finite expression for the total hadronic cross section in the threshold limit $s\to 4m^2$. This effect can be attributed to the Coulomb singularity caused by the exchange of massless gauge bosons between massive fermions. We will come back to this point in the next section.

Another observation we want to bring to the attention of the reader is that the leading cutoff term $\ln^2\delta$ appearing in (6.19) [see also (D1) and (D2)] is proportional to the Born cross section in (2.17). This is in agreement with the work of Mueller and Nason[31] who assumed that the leading soft-gluon terms in heavy flavor production form

the exponential series $\exp[(2\alpha_s N \ln^2\delta)/\pi]$.

Finally we have the heavy-fermion-loop contribution to (6.19):

$$s^2\left[\frac{d^2\hat{\sigma}^{(1)}_{gg,f}}{dt_1 du_1}\right]^{V+S} = \sum_{f=H,L} \tfrac{1}{16}\alpha_s^3 K C_O F_f^{V+S}(t,u,t_1,u_1) \times \delta(s+t_1+u_1) - \frac{\alpha_s}{2\pi}\sum_{f=H}\tilde{\beta}_{0,f}\ln\frac{m_f^2}{m^2}s^2\left[\frac{d\hat{\sigma}^{(0)}_{gg}}{dt_1 du_1}\right], \tag{6.21}$$

where the summation is over the heavy ($H=c,b,t$) and/or light ($L=u,d,s$) quark contributions. The last term in (6.21) contains the Born cross section in (2.14). For $s>4m_f^2$, F_H^{V+S} is given by

$$F_H^{V+S}=(t_1-u_1)^2 \times\left[-\frac{2m^2m_f^2}{s^2t_1u_1}[8-6\zeta(2)+4r_f\ln x_f+\ln^2 x_f] - \frac{2}{3}\frac{m^2}{st_1u_1}\right], \tag{6.22}$$

where

$$r_f=(1-4m_f^2/s)^{1/2},\quad x_f=\frac{1-r_f}{1+r_f}. \tag{6.23}$$

For $s<4m_f^2$, F_H^{V+S} is given by

$$F_H^{V+S}=(t_1-u_1)^2 \times\left[-\frac{2m^2m_f^2}{s^2t_1u_1}(8-8\bar{r}_f\arctan\bar{x}_f-4\arctan^2\bar{x}_f) - \frac{2}{3}\frac{m^2}{st_1u_1}\right], \tag{6.24}$$

where

$$\bar{r}_f=(4m_f^2/s-1)^{1/2},\quad \bar{x}_f=\frac{1}{\bar{r}_f}. \tag{6.25}$$

In the case of the light u,d,s quarks the last term in (6.21) is removed by mass factorization [see (6.7)] and F_L^{V+S}, which no longer contains the mass of the light quarks, is

$$F_L^{V+S}=-\frac{2}{3}\frac{m^2(t_1-u_1)^2}{st_1u_1}. \tag{6.26}$$

The renormalization of the fermion-loop contribution in (6.21) differs from that used in Ref. 13, where the renormalization scheme was chosen in such a way that no logarithms of the type $\ln(m_f^2/Q^2)$ (with Q the mass factorization scale) appear in the renormalized cross section. In such a scheme one invokes the decoupling theorem so that light ($m_f^2<Q^2$) as well as heavy ($m_f^2>Q^2$) fermions are simply removed from the perturbative expansion. However, we prefer to let field theory take care of its own large corrections. This is the case in the first part of (6.21) where the expression F_f^{V+S} is well behaved for small as well as large m_f^2/s. However, the logarithmic terms in the second part of (6.21) are appreciable if Q^2 ($=m^2$) is much larger or much smaller than m_f^2. In the former case one gets a negative contribution while in the latter case a positive one. The source of these logarithms is the self-energy insertion in the external gluon legs. In calculating the hadronic cross sections (see Sec. VII) we shall adopt the convention that the number of active flavors n_f in the running coupling constant and in the internal fermion loops should never exceed the rank of the produced flavor in the final state. This implies that for c-, b-, and t-quark production we only include four, five, and six internal (active) flavors, respectively. Since the factorization scale is of the order of the produced heavy-quark mass m the heavy fermions with $m_f>m$ are automatically decoupled from our hadronic cross section. Therefore we only have to deal with the situation that $Q(=m)>m_f$. In the case of t-quark production the size of the logarithmic terms $\ln(m_f^2/m_t^2)$ where ($f=c,b$; $Q=m=m_t$) is noticeable (about 20% of the cross section, see Sec. VII). Therefore one has to resum these large logarithms which can be done by replacing the running coupling constant in the gluon-gluon-fusion cross section by

$$\hat{\alpha}_s(Q)^{-1}=\alpha_s(Q)^{-1} \times\left[1+[\alpha_s(Q)/4\pi]\sum_{f=H}\tilde{\beta}_{0,f}\ln(m_f^2/Q^2)\right]. \tag{6.27}$$

The unrenormalized virtual cross section in (3.5) can be reconstructed from the reduced virtual plus soft cross sections in (D1)–(D3) and (6.21) in a straightforward way. First, we subtract the soft cross section (5.6) from the reduced cross section in (6.9). In this way one obtains the renormalized virtual cross section on the left-hand side of (3.13). The unrenormalized one (with respect to the coupling-constant renormalization) follows from the right-hand side of the last equation.

Before finishing this section we would like to comment on the regularization dependence of the reduced cross section. In particular we want to discuss the result which follows from using n-dimensional reduction rather than n-dimensional regularization for the parton cross sections. One has to be careful using n-dimensional reduction in order to regulate the UV divergences.[32] Since it is very hard to disentangle the UV divergences from the IR and collinear singularities in the virtual amplitudes (3.6) we limit ourselves to the collinear divergences which appear in the hard-gluon cross section. If we assume that the reduced hard cross section is regularization independent then one can derive the following relation from (6.9):

$$s^2\frac{d^2\sigma'^{(1)}_{gg}(s,t_1,u_1)}{dt_1du_1}=s^2\frac{d^2\sigma^{(1)}_{gg}(s,t_1,u_1)}{dt_1du_1}$$
$$+\frac{\alpha_s}{2\pi}\left[\int_0^{1-\delta_1}\frac{dx_1}{x_1}\frac{2}{\epsilon}P^H_{gg}(x_1)\left[\hat{s}^2\frac{d^2\sigma'^{(0)}_{gg}(x_1s,x_1t_1,u_1)}{d\hat{t}_1du_1}-\hat{s}^2\frac{d^2\sigma^{(0)}_{gg}(x_1s,x_1t_1,u_1)}{d\hat{t}_1du_1}\right]\right.$$
$$+\int_0^{1-\delta_2}\frac{dx_2}{x_2}\frac{2}{\epsilon}P^H_{gg}(x_2)\left[\hat{s}^2\frac{d^2\sigma'^{(0)}_{gg}(x_2s,t_1,x_2u_1)}{dt_1d\hat{u}_1}-\hat{s}^2\frac{d^2\sigma^{(0)}_{gg}(x_2s,t_1,x_2u_1)}{dt_1d\hat{u}_1}\right]$$
$$+\int_0^{1-\delta_1}\frac{dx_1}{x_1}[f^{H'}_{gg}(x_1,Q^2,\mu^2)-f^H_{gg}(x_1,Q^2,\mu^2)]\hat{s}^2\frac{d^2\sigma^{(0)}_{gg}(x_1s,x_1t_1,u_1)}{d\hat{t}_1du_1}$$
$$\left.+\int_0^{1-\delta_2}\frac{dx_2}{x_2}[f^{H'}_{gg}(x_2,Q^2,\mu^2)-f^H_{gg}(x_2,Q^2,\mu^2)]\hat{s}^2\frac{d^2\sigma^{(0)}_{gg}(x_2s,t_1,x_2u_1)}{dt_1d\hat{u}_1}\right]. \quad (6.28)$$

Here the prime means that we have calculated the quantities by using n-dimensional reduction whereas the unprimed quantities are calculated by n-dimensional regularization. Notice that $d\sigma'^{(0)}-d\sigma^{(0)}$ is of order ϵ; therefore we can neglect the difference if $d\sigma'^{(0)}$ and $d\sigma^{(0)}$ are multiplied by finite functions. $P^H_{gg}(x)$ is a universal function independent of the regularization method. However f^H_{gg} and $f^{H'}_{gg}$ depend on the regularization scheme. In order to perform the mass factorization we have to define them in another process. This can be any process provided it shows the same collinear divergences. Here we choose the reaction

$$g+g\rightarrow s+g\ , \quad (6.29)$$

where s is a scalar which is a singlet under the local gauge group. The gauge-invariant interaction Lagrangian is given by

$$\mathcal{L}_{\rm int}(x)=\lambda\phi(x)G^a_{\mu\nu}(x)G^{a\mu\nu}(x)\ , \quad (6.30)$$

where $\phi(x)$ is an external source and we work in lowest order in λ and (in principle) in all orders of the gauge-coupling constant. Our findings are that $f^H_{gg}=f^{H'}_{gg}$ so that the difference between $d\sigma'^{(1)}$ and $d\sigma'^{(0)}$ only originates from the difference between the Born cross sections $d\sigma'^{(0)}$ and $d\sigma^{(0)}$. We discovered that relation (6.28) holds if we put the quark masses equal to zero. However, this relation does not hold for the terms proportional to m^2 and m^4. This means that for the n-dimensional reduction method we would not have found all the m^2 and m^4 terms in the contributions between the large square brackets in (6.28). The situation can only be rectified if we assume that in n-dimensional reduction the function $f^{H'}_{gg}$ gets an additional part which is equal to

$$f'^H_{gg}(x)=-2N\frac{1-x}{x}\ , \quad (6.31)$$

provided this term is only convoluted with the mass terms in the Born section $d\sigma^{(0)}_{gg}$ in (6.28) and not with the massless part. This is of course ugly and it means that something is wrong with n-dimensional reduction or with mass factorization.

For the moment we can conclude that the regularization independence of the reduced hard-gluon cross section only works for the massless parts. It breaks down for terms which are proportional to the quark mass m^2. We have also checked this statement for the reactions $q+\bar{q}\rightarrow W+\gamma+g$, and $q(\bar{q})+g\rightarrow W+\gamma+q(\bar{q})$ in Ref. 26 where the W is massive but the quarks and gluons are massless. In these cases the reduced hard-gluon cross sections are independent of the regularization method used. Hence it is the quark masses which are responsible for the difference between n-dimensional reduction and n-dimensional regularization.

VII. HEAVY-FLAVOR PRODUCTION

In this section we will discuss the total and differential cross sections of t- and b-quark production via the gluon-gluon-fusion mechanism in (1.2). Besides t and b production we could also study c production, but since m_c is much smaller than the collider energy we believe that the c quark should be treated as a light quark rather than a heavy one. In this paper we present the results of our calculations for representative values of the input parameters. The hadronic reaction in which the heavy flavors are produced is given by

$$p(P_1)+\bar{p}(P_2)\rightarrow Q(p_1)+\bar{Q}(p_2)+X\ , \quad (7.1)$$

where p and $\bar{p}$ denote the proton and antiproton, respectively. The quantity X stands for all final hadronic states which we sum over so that the above process is inclusive with respect to the outgoing hadrons. We use capital letters for the momenta and invariants of the proton and antiproton to distinguish them from those of the quarks and gluons. These invariants are [see (4.10)]

$$S=(P_1+P_2)^2\ ,$$
$$T_1=(P_2-p_2)^2-m^2\ , \quad (7.2)$$
$$U_1=(P_1-p_2)^2-m^2\ ,$$

where S denotes the square of the hadron c.m. energy and T_1,U_1 are the hadronic analogues of t_1,u_1 in (4.2). The hadronic cross section for the process in (7.1) reads

$$S^2\frac{d^2\sigma(S,T_1,U_1)}{dT_1dU_1}=\int_{x_{1-}}^1\frac{dx_1}{x_1}\int_{x_{2-}}^1\frac{dx_2}{x_2}H_{gg}(x_1,x_2,Q^2)\times s^2\frac{d^2\hat{\sigma}_{gg}(s,t_1,u_1)}{dt_1du_1}\ . \tag{7.3}$$

The lower limits x_{1-},x_{2-} are defined in (4.12) (see also Fig. 5). $d^2\hat{\sigma}_{gg}$ denotes the reduced (mass factorized) parton cross section which has been calculated up to order α_s^3 in the previous section. H_{gg} is the product of the scale-dependent gluon distribution functions. It is given by [see (4.10)]

$$H_{gg}(x_1,x_2,Q^2)=f_g^p(x_1,Q^2)f_g^{\bar{p}}(x_2,Q^2)\ , \tag{7.4}$$

where f_g^p, $f_g^{\bar{p}}$ denote the gluon distribution functions of the proton and antiproton, respectively, which can be set equal to each other.

For the gluon distribution function we have chosen the EHLQ parametrization, with $Q_0=2$ GeV/c and $\Lambda=0.2$ GeV/c (Ref. 33). This choice implies $f_g(x,Q_0^2)\sim x^{-1}$ for small x. The running coupling constant is given by

$$\alpha_S(Q^2)=\frac{12\pi}{(33-2n_f)\ln Q^2/\Lambda^2}\ . \tag{7.5}$$

Furthermore, we will take $Q^2=m^2$ as the mass factorization scale in the gluon distribution function as well as in the running coupling constant α_s. As we have already mentioned below (6.13), there is an uncertainty in the expression for the gluon distribution function. This holds for its x dependence as well as its higher-order QCD corrections. The latter depends on the chosen mass factorization scheme. Neither deep-inelastic lepton hadron scattering nor direct photon production ($p+\bar{p}\to\gamma+X$) provides us with sufficient high-statistics data needed for an accurate determination of the gluon distribution function. Therefore the contribution of the gluon-gluon fusion mechanism to the hadronic reaction in (7.1) will heavily depend on the chosen mass factorization scheme and the uncertainty in the large-x behavior of the parametrization in the gluon distribution function.

Denoting the gluon-gluon Born cross section (2.14) by the shorthand notation

$$s^2\frac{d^2\hat{\sigma}_{gg}^{(0)}}{dt_1du_1}=\delta(s+t_1+u_1)\sigma_{gg}^{(0)}(s,t_1,u_1)\ , \tag{7.6}$$

its contribution to the hadronic cross section (7.3) can be written as

$$\left[S^2\frac{d^2\sigma(S,T_1,U_1)}{dT_1dU_1}\right]^B=\int_{x_{1-}}^1\frac{dx_1}{x_1}\left[-\frac{1}{x_1T_1}\right]H_{gg}\left[x_1,-\frac{x_1T_1}{x_1S+U_1},m^2\right]\times\sigma_{gg}^{(0)}\left[-\frac{x_1^2T_1}{x_1S+U_1}S,x_1T_1,-\frac{x_1T_1}{x_1S+U_1}U_1\right], \tag{7.7}$$

with x_{1-} given in (4.12).

Following the discussion below (4.12) we split the order-α_s correction to the Born hadronic cross section into a virtual plus soft- and a hard-gluon part. The virtual plus soft contribution, which is given in (6.19), can be denoted by

$$\left[s^2\frac{d\hat{\sigma}_{gg}^{(1)}}{dt_1du_1}\right]^{V+S}=\delta(s+t_1+u_1)\sigma_{gg}^{V+S}(s,t_1,u_1,\Delta)\ . \tag{7.8}$$

The virtual plus soft part of the hadronic cross section therefore equals

$$\left[S^2\frac{d^2\sigma(S,T_1,U_1)}{dT_1dU_1}\right]^{V+S}=\int_{x_{1-}}^1\frac{dx_1}{x_1}\left[-\frac{1}{x_1T_1}\right]H_{gg}\left[x_1,-\frac{x_1T_1}{x_1S+U_1},m^2\right]\times\sigma_{gg}^{V+S}\left[-\frac{x_1^2T_1}{x_1S+U_1}S,x_1T_1,-\frac{x_1T_1}{x_1S+U_1}U_1,\Delta\right]. \tag{7.9}$$

The hard-gluon correction term is given by (6.15). The hard-gluon part of the hadronic cross section reads

$$\left[S^2\frac{d^2\sigma(S,T_1,U_1)}{dT_1dU_1}\right]^H=\int_{x_{1-}}^1\frac{dx_1}{x_1}\int_{x_{2-}^*}^1\frac{dx_2}{x_2}H_{gg}(x_1,x_2,m^2)\left[s^2\frac{d\hat{\sigma}_{gg}^{(1)}}{dt_1du_1}(x_1x_2S,x_1T_1,x_2U_1)\right]^H, \tag{7.10}$$

where x_{2-}^* is determined by the condition [see (4.11)]

$$s_4=x_1x_2S+x_1T_1+x_2U_1>\Delta\ , \tag{7.11}$$

which yields (see also Fig. 5)

$$x_{2-}^*=(\Delta-x_1T_1)/(x_1S+U_1)\ . \tag{7.12}$$

Other differential cross sections such as, e.g., $d^2\sigma/dy\,dp_T$, where y is the rapidity, can be obtained from the above expressions by multiplying by the appropriate Jacobians. The total cross section for (7.1) is

$$\sigma_{\rm tot}=\int_{(S-\bar{S})/2}^{(S+\bar{S})/2}d(-T_1)\times\int_{-Sm^2/T_1}^{S+T_1}d(-U_1)\frac{d^2\sigma(S,T_1,U_1)}{dT_1dU_1}\ , \tag{7.13}$$

where $\bar{S}=S\sqrt{1-4m^2/S}$ and the pieces of $d^2\sigma$ are given by Eqs. (7.7), (7.9), and (7.10), respectively. Expression (7.13) can also be inferred from the reduced parton cross section $d\hat{\sigma}$ since

$$\sigma_{\rm tot}=\int_{4m^2/S}^{1}dx_1\int_{4m^2/x_1S}^{1}dx_2 H_{gg}(x_1x_2m^2)\times\hat{\sigma}(x_1x_2S,m^2)\ , \qquad (7.14)$$

where $\hat{\sigma}(s,m^2)$ is defined by

$$\hat{\sigma}(s,m^2)=\int_{(s-\bar{s})/2}^{(s+\bar{s})/2}d(-t_1)\times\int_{-sm^2/t_1}^{s+t_1}d(-u_1)\frac{d^2\hat{\sigma}(s,t_1,u_1)}{dt_1du_1}\ . \qquad (7.15)$$

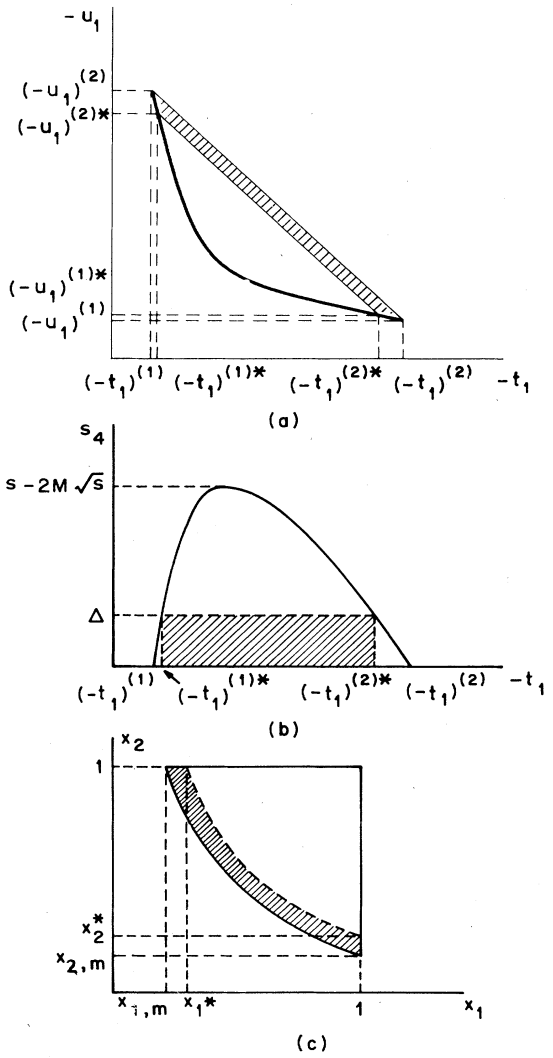

FIG. 5. The Dalitz plot for the $P+\bar{P}\to Q+\bar{Q}+X$. (a) shows $-u_1$ versus $-t_1$, where the points marked are $(-t_1)^{(1)*}=(-u_1)^{(1)*}=\frac{1}{2}(s-\sqrt{s^2-4sm^2})(1+\Delta/\sqrt{s^2-4sm^2})$, $(-t_1)^{(2)*}=(-u_1)^{(2)*}=\frac{1}{2}(s+\sqrt{s^2-4sm^2})(1-\Delta/\sqrt{s^2-4sm^2})$. $(-t_1)^{(1)}=(-u_1)^{(1)}$ and $(-t_1)^{(2)}=(-u_1)^{(2)}$ are obtained from $(-t_1)^{(1)*}$, $(-t_1)^{(2)*}$ by putting $\Delta=0$. (b) shows s_4 vs $-t_1$. (c) shows x_2 vs x_1 where the points marked are $x_1^*=(\Delta-U_1)/(S+T_1)$, $x_2^*=(\Delta-T_1)/(S+U_1)$. $x_{1,m}$ and $x_{2,m}$ are obtained from x_1^* and x_2^* by putting $\Delta=0$. The hatched area represents the soft-gluon part of the Dalitz plot.

The integration boundaries are indicated in the Dalitz plot of Fig. 5. Notice that for $d\hat{\sigma}^H$ the upper boundary in the u_1 integral has to be replaced by $s+t_1-\Delta$. The integrations have been carried out numerically by using VEGAS (Ref. 34). We checked that (7.13) and (7.14) are numerically equal.

Let us first consider our results for the parton-parton subprocess. Because of the fermion-loop contribution to $d\hat{\sigma}^{V+S}$ in (6.21), $\hat{\sigma}$ depends on the internal fermion mass m_f which takes the values of the heavy flavor masses of the c, b, and t quarks. The mass of the internal flavor quark m_f is not necessarily equal to the corresponding mass of the heavy flavor quark produced in the final state (denoted by m). In order to compare with the results of Ref. 13 we omit for the moment the logarithmic terms of the type $\ln(m_f^2/m^2)$ in the second part of (6.21) [cf., the discussion after (6.27)]. The remaining part of the fermion-loop contribution is very small due to the decoupling mechanism. Therefore one can write the perturbative expansion of the parton cross section in terms of scaling functions,[13] i.e.,

$$\hat{\sigma}_{gg}(s,m^2)=\frac{\alpha_s^2(m^2)}{m^2}[f_{gg}^{(0)}(\rho)+4\pi\alpha_s(m^2)f_{gg}^{(1)}(\rho)] \qquad (7.16)$$

where $f_{gg}^{(0)}, f_{gg}^{(1)}$ stand for the Born contribution to the gluon-gluon-fusion mechanism, and the order-α_s correction, respectively, and $\rho=4m^2/s$. Notice that in contrast with Ref. 13 we have already put the mass factorization scale Q^2 to be equal to m^2. In Figs. 6 and 7 we present the various contributions to (7.16). For that purpose we have split the order-α_s correction into a virtual plus soft part (6.19) [including the first part of the fermion-loop contribution in (6.21)] and a hard-gluon part (6.15). For

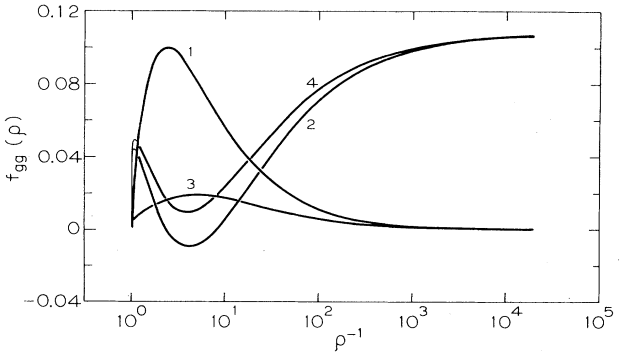

FIG. 6. Plot of the scaling functions $f_{gg}^{(0)}(\rho)$ and $f_{gg}^{(1)}(\rho)$ appearing in (7.16). (1) $f_{gg}^{(0)}(\rho)$, Born term. (2) $f_{gg}^{(1)}(\rho)$, hard-gluon part. (3) $f_{gg}^{(1)}(\rho)$, virtual+soft-gluon part. (4) $f_{gg}^{(1)}(\rho)$, hard+virtual+soft.

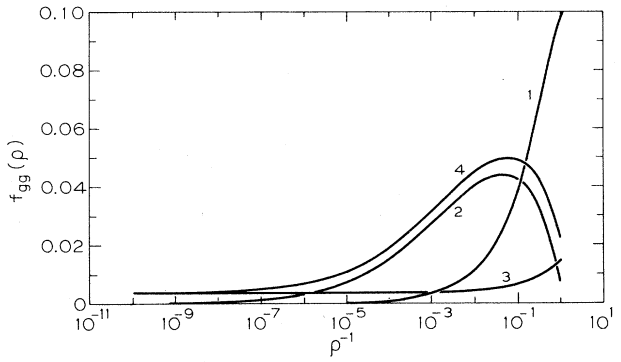

FIG. 7. Plot of the scaling functions $f_{gg}^{(0)}(\rho)$ and $f_{gg}^{(1)}(\rho)$ appearing in (7.16). (1) $f_{gg}^{(0)}(\rho)$, Born term. (2) $f_{gg}^{(1)}(\rho)$, hard-gluon part. (3) $f_{gg}^{(1)}(\rho)$, virtual+soft-gluon part. (4) $f_{gg}^{(1)}(\rho)$, hard +virtual+soft.

the number of flavors we took $n_f=6$. Note that in the subsequent presentation of our results for the cross sections we have removed the $\ln\Delta$ terms from the virtual plus soft contribution and added them to the hard-gluon part. We then checked that the new hard piece was independent of Δ as $\Delta\to 0$.

Our results for $f_{gg}^{(1)}$ agree with those found in Ref. 13 for the whole range of ρ. From Figs. 6 and 7 we infer that for $1.1<\rho^{-1}<10$ the Born process (1.2) dominates over the order-α_s correction, whereas for $\rho^{-1}<1.1$ and $\rho^{-1}>10$ the inverse is true. Furthermore, Fig. 6 reveals that the virtual plus soft contribution is smaller than the hard-gluon part ($\ln\Delta$ terms from the virtual plus soft included) except in the region $2<\rho^{-1}<12$. Notice that for the comparison between the Born and the order-α_s correction one has to bear in mind that the function $f_{gg}^{(1)}$ has to be multiplied by $4\pi\alpha_s(m^2)\sim 2$. The large contribution of the order-α_s correction to process (1.4) in the region $\rho^{-1}>10$ is wholly due to the hard-gluon part and can be traced back to the s_5 channel poles (4.2) appearing in $d\hat{\sigma}_{gg,O}^{H}$ in (6.16). This effect can be explained by the exchange of a gluon in the t channel of the subprocess $g+g\to g+g^*$ with $g^*\to Q\bar{Q}$. This subprocess contributes to $d\hat{\sigma}_{gg,O}^{H}$ only and dominates in the high-energy limit. Near threshold $\rho^{-1}<1.1$ the dominance of the order-α_s correction can be attributed to soft-gluon radiation coming from the expressions $d\hat{\sigma}_{gg,O}^{H}$ and $d\hat{\sigma}_{gg,K}^{H}$ in (6.16) and (6.17), respectively. For $\rho^{-1}\sim 1$ the threshold behavior of the cross section in (7.16) can be exactly calculated from the expressions given in Appendix D. In the limit that $s\to 4m^2$ we obtain

$$\hat{\sigma}_{gg}(s,m^2)=\pi\alpha_s^2\frac{K}{s}\left[C_O\tfrac{1}{2}\beta-C_K\beta+C_{\mathrm{QED}}\beta+\frac{\alpha_s}{\pi}NC_O[\beta\ln^2(8\beta^2)-\tfrac{9}{2}\beta\ln(8\beta^2)]\right.$$
$$\left.+\frac{\alpha_s}{\pi}NC_K[-\tfrac{1}{8}\pi^2-2\beta\ln^2(8\beta^2)+10\beta\ln(8\beta^2)]+\frac{\alpha_s}{\pi}\bar{C}_{\mathrm{QED}}\frac{\pi^2}{4}\right], \tag{7.17}$$

with $\beta=\sqrt{1-\rho}$. In the case of QCD ($N=3$) the above expression agrees with that given in (26) of Ref. 13. It describes the threshold behavior of $\hat{\sigma}_{gg}$ very well for values of $\rho^{-1}<1.0001$. Furthermore, we infer from the above result that at threshold the Born cross section equals zero whereas the order-α_s correction becomes a constant. This is due to the Coulomb singularity present in $d\hat{\sigma}_{K}^{V+S}$ and $d\hat{\sigma}_{\mathrm{QED}}^{V+S}$ which leads to the π^2 terms in (7.17). The threshold behavior of the parton cross section of the gluon-gluon-fusion process is very important for the hadronic cross section. Since the gluon distribution function increases very steeply at small x values the main part of the hadronic cross section is determined by the threshold behavior of the parton cross section ($s=x_1x_2S$). Finally, we infer from Ref. 13 that the order-α_s correction to the gluon-gluon-fusion process dominates over the other heavy-flavor production mechanisms such as (1.3) and (1.5) not discussed in this paper.

In the next figures we show the parton cross section (7.15) evaluated for charm ($m_c=1.5$ GeV/c^2), bottom ($m_b=5.0$ GeV/c^2), and top-quark production ($m_t=40$ GeV/c^2). Here we also include the logarithms in the second part of (6.21). Furthermore we use the running coupling constant in (7.5). In the case of c-quark production in Fig. 8 we use four active flavors only for the running coupling constant ($\alpha_s=0.37$) as well as for the internal fermion-loop contribution (6.21). This implies that the heavy fermions with $m_f>m_c$ decouple from the virtual contribution [see the discussion after (6.26)]. In Fig.

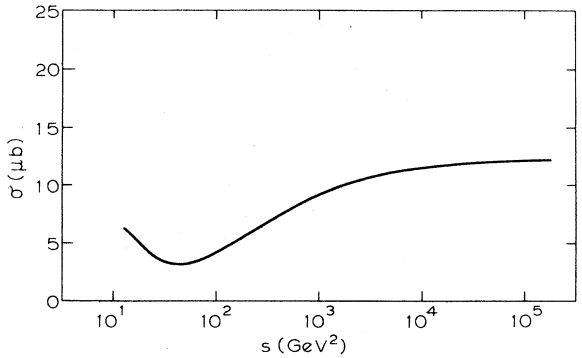

FIG. 8. Total parton cross section for charm production with $n_f=4$ flavors in the internal fermion-loop contribution and the running coupling constant.

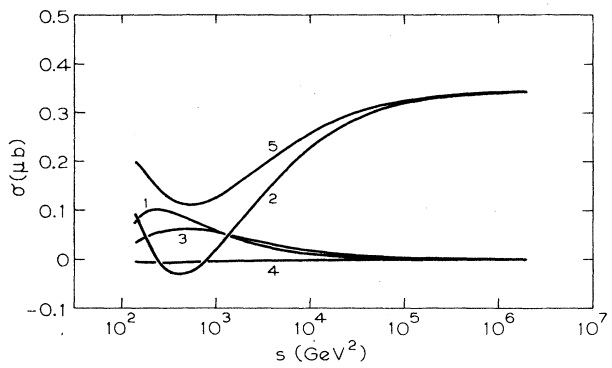

FIG. 9. Total parton cross section for b-quark production ($n_f=5$). (1) Born term. (2) Hard-gluon part. (3) Virtual-soft-gluon part. (4) Fermion loop. (5) Sum of 1–4.

9 we show the parton cross section for b production. Here we take five active flavors ($\alpha_S=0.255$) which leads to a small contribution from logarithmic terms of the type $\ln(m_f^2/m_b^2)$ for $m_f<m_b$ (here only m_c is relevant). Furthermore, we have split the total parton cross section into its various parts: i.e., Born, virtual plus soft (without the fermion loop), fermion loop and hard gluon (including the $\ln\Delta$ terms from the virtual plus soft). The various contributions follow the pattern already discussed for $f_{gg}^{(1)}(\rho)$ in (7.16). The same contributions are shown in Fig. 10 for the parton cross section for t-quark production. Here we have chosen six active flavors ($\alpha_s=0.169$). It appears that the contributions of the logarithms $\ln(m_f^2/m_t^2)$ to the fermion-loop contributions are much larger than in the previous case (here both m_c and m_b are relevant). These terms contribute about 20% of the hadronic cross section, so we have to resum them in order to make reliable predictions.

We now give a sample of results for the hadronic cross sections for b as well as t-quark production including the differential distributions with respect to p_T (transverse momentum) and y (rapidity). Since we have numerically stable values for the total cross sections (accurate to at least 1%), we simply chose a small value for Δ and integrated the original virtual plus soft contribution and

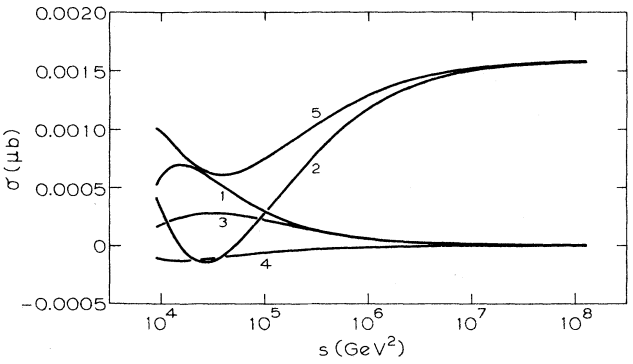

FIG. 10. Total parton cross section for t-quark production ($n_f=6$). (1) Born term. (2) Hard-gluon part. (3) Virtual-soft-gluon part. (4) Fermion loop. (5) Sum of 1–4.

TABLE I. Total $p\bar{p}$ cross section (all units in μb) for b-quark production $m_b=5.0\text{GeV}/c^2$, $\alpha_s(m_b)=0.255$ ($q\bar{q}$), $\bar{\alpha}_s(m_b)=0.247$ (gg), and $n_f=5$ in (6.21) and (7.5).

$\sqrt{S}$ (TeV)	$q\bar{q}O(\alpha_s^2)$	$ggO(\alpha_s^2)$	$ggO(\alpha_s^3)$
0.63	0.39	8.9	11
1.8	0.55	26	40

the hard contribution separately, plotting all the relevant distributions. We then checked that the addition of the two pieces produced stable results, after cancellations of at least 1 order of magnitude, and the correct value for the total cross section. The cancellations occur all over the phase space so a considerable amount of computer time was required to stabilize the final values in all the bins in p_T and y. However, the final distributions are good to about 5%. We concentrate on getting accurate theoretical results for $p\bar{p}$ collisions at $\sqrt{S}=0.63$ and 1.8 TeV. For the input parton distribution functions we chose the EHLQ parametrization.[33]

The total $p\bar{p}$ cross sections for b ($m_b=5.0$ GeV/c^2) and t ($m_t=40.0$ GeV/c^2, and $m_t=80.0$ GeV/c^2) production are presented in Tables I and II, respectively. The results for the order-α_s^2 and the order-α_s^3 contribution to the gluon-gluon-fusion processes are shown separately. We have also included the cross section for the order-α_s^2, $q\bar{q}$ fusion process (1.1), using the EHLQ quark-antiquark structure functions, since it is relevant for t-quark production. For b-quark production we have chosen five active flavors ($n_f=5$). In the case of the $q\bar{q}$ fusion process we took the running coupling constant $\alpha_s(m^2)$ given by (7.5) ($\alpha_s=0.255$). However, for the gluon-gluon-fusion process we have to resum the logarithms of the type $\ln(m_f^2/m^2)$ which can be achieved via the replacement of α_s by $\bar{\alpha}_s$ in (6.27), ($\bar{\alpha}_s=0.247$). This replacement will only introduce a minor correction in the case of b production. For t production we have chosen six active flavors ($n_f=6$). Further we proceed in the same way as in the case of b production. For the $q\bar{q}$ fusion process we take $\alpha_s=0.169$ ($m_t=40.0$ GeV/c^2), and for the gluon-gluon-fusion process we choose $\bar{\alpha}_s=0.155$, ($m_t=40.0$ GeV/c^2). Changing α_s into $\bar{\alpha}_s$ will decrease the gluon-gluon cross section by about 20%. If $m_t=80.0$ GeV/c^2 the values for α_s and $\bar{\alpha}_s$ become 0.150 and 0.135, respectively. From Tables I and II we infer that the α_s^3 cross section is a significant fraction of the total for these masses and energies. This could already be expected from the input parton cross sections as has been dis-

TABLE II. Total $p\bar{p}$ cross section (all units in nb) for t-quark production, $\alpha_s(40)=0.169(q\bar{q})$, $\bar{\alpha}_s(40)=0.155(gg)$; $\alpha_s(80)=0.150(q\bar{q})$, $\alpha_s(80)=0.135$ (gg); and $n_f=6$ in (6.21) and (7.5).

m_t (GeV/c^2)	$\sqrt{S}$ (TeV)	$q\bar{q}O(\alpha_s^2)$	$ggO(\alpha_s^2)$	$ggO(\alpha_s^3)$
40.0	0.63	0.54	0.39	0.38
40.0	1.8	1.9	10	7.7
80.0	0.63	0.016	0.0011	0.0014
80.0	1.8	0.17	0.23	0.18

TABLE III. Total $p\bar{p}$ cross section (all units in μb) for b-quark production $m_b=5.0$ GeV/c^2, $\alpha_s(m_b)=0.190$ for both $q\bar{q}$ and gg, and $n_f=5$ in (6.21) and (7.5); see Ref. 14.

$\sqrt{S}$ (TeV)	$q\bar{q}O(\alpha_s^2)$	$ggO(\alpha_s^2)$	$ggO(\alpha_s^3)$
0.63	0.22	5.3	5.0
1.8	0.31	16	18

cussed above. Comparison with the literature reveals that the values for the b and t production cross sections as quoted in our tables are larger than those of other authors[1,14] due to our choice of the running coupling constant.

If we want to make a comparison with Ref. 14 one has to use the renormalization scheme where all heavy fermions are decoupled from the radiative corrections. As discussed after (6.26) this implies that the second part of (6.21), which contains the logarithmic terms $\ln(m_f^2/m^2)$ have to be removed from the fermion-loop contribution. Furthermore, we use the two-loop corrected running coupling constant as given in (10) in Ref. 14 with $\Lambda=0.17$ GeV/c^2 and factorization scale $Q=m$. The values of the running coupling constant for b and t production are 0.190 and 0.125 ($m_t=40.0$ GeV/c^2) and 0.112 ($m_t=80.0$ GeV/c^2), respectively. Furthermore, the number of flavors in both cases was chosen to be $n_f=5$. The values for the b and t production cross sections are presented in Tables III and IV, respectively. From these tables we infer that there exists an agreement between our results and those given in Table II of Ref. 14. The small discrepancies are due to the fact that we have not calculated the small contributions from the processes (1.3) and (1.5). To further check our numbers we used the expression for $f_{gg}^{(1)}(\rho)$ [in (23) in Ref. 13]. We were able to reproduce our numbers in Tables I–IV to within 1%. In addition we computed for t-quark production ($m_t=40.0$ GeV/$c^2\sqrt{S}=0.63$ TeV) the ratio of the order-α_s correction divided by the Born cross section which in our case is about 1.5 ($\alpha_s=0.158$). The last number is in agreement with Fig. 14 in Ref. 13.

The differential cross sections with respect to p_T and y which are shown in the subsequent figures are computed with the same two-loop corrected running coupling constant and the renormalization scheme as used in Ref. 14. Here both the gluon-gluon-fusion mechanism and the Born cross section for the $q\bar{q}$ reaction have been taken into account. Since the cross sections for the Born and the order-α_s contributions are almost equal in magnitude

TABLE IV. Total $p\bar{p}$ cross section (all units in nb) for t-quark production, $\alpha_s(40)=0.125$, $\alpha_s(80)=0.112$ for both $q\bar{q}$ and gg, and $n_f=5$ in (6.21) and (7.5); see Ref. 14.

m_t (GeV/c^2)	$\sqrt{S}$ (TeV)	$q\bar{q}$ $O(\alpha_s^2)$	$ggO(\alpha_s^2)$	$ggO(\alpha_s^3)$
40.0	0.63	0.29	0.26	0.21
40.0	1.8	1.03	6.5	4.1
80.0	0.63	0.009	0.0008	0.0008
80.0	1.8	0.095	0.16	0.10

it is best to separately display the distributions for the Born cross section and the total cross section. Figure 11 shows the p_T distribution for the b quark with mass 5 GeV/c^2 in the reaction $p+\bar{p}\to b+\bar{b}+X$ in order α_s^2 and α_s^3 at $\sqrt{S}=0.63$ TeV. The same distributions are plotted in Fig. 12 for $\sqrt{S}=1.8$ TeV. In Fig. 13 we show the p_T distribution for the t quark in the reaction $p+\bar{p}\to t+\bar{t}+X$ with mass $m_t=40.0$ GeV/c^2 for $\sqrt{S}=1.8$ TeV. These results show that the radiatively corrected p_T distributions are uniformly larger than those of the Born approximation. Since the cross section is largest for s near threshold both the virtual plus soft and the hard parts contribute. In Figs. 14–16 we also present the rapidity distributions for the b and t quarks choosing the same parameters as given above. The corrections are again uniformly positive and primarily change the height of the distribution.

Notice that our results for the p_T and y distributions cannot directly be compared to those from Ali, van Eijk, and ten Have in Ref. 3. These authors implemented a p_T cut on the hard-gluon radiation cross section in order to avoid the collinear singularities arising in the matrix element. The correction they obtained therefore had to be positive. Mass factorization removes this singular part from the cross section so it is not obvious what the correct results should be. The QCD corrections in this paper are obtained from an exact calculation.

The UA1 group[2] have recently presented their data for b-quark production at $\sqrt{S}=0.63$ TeV, in the form of a differential distribution in $p_T>p_T^{\min}$ with an experimental

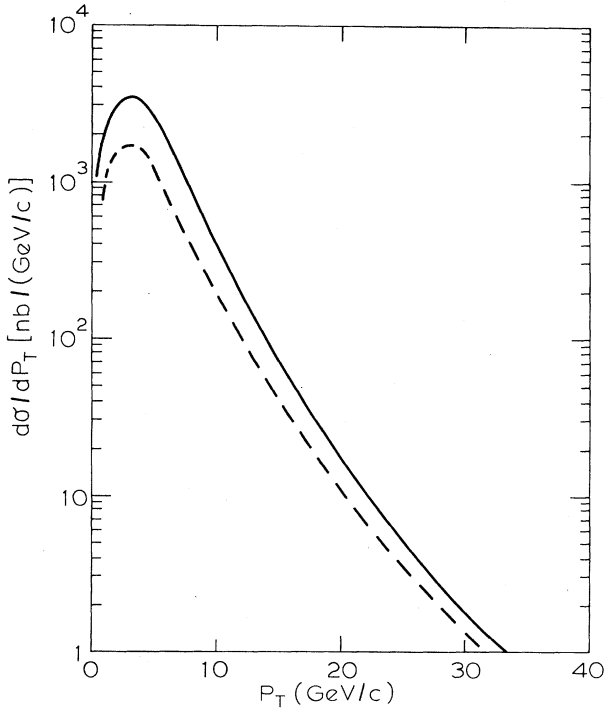

FIG. 11. $d\sigma/dp_T$ for b-quark production ($m_b=5.0$ GeV/c^2) at $\sqrt{S}=0.63$ TeV. Dashed line: $O(\alpha_s^2)$ cross section; solid line: sum of the $O(\alpha_s^2)$ cross section and the $O(\alpha_s^3)$ correction.

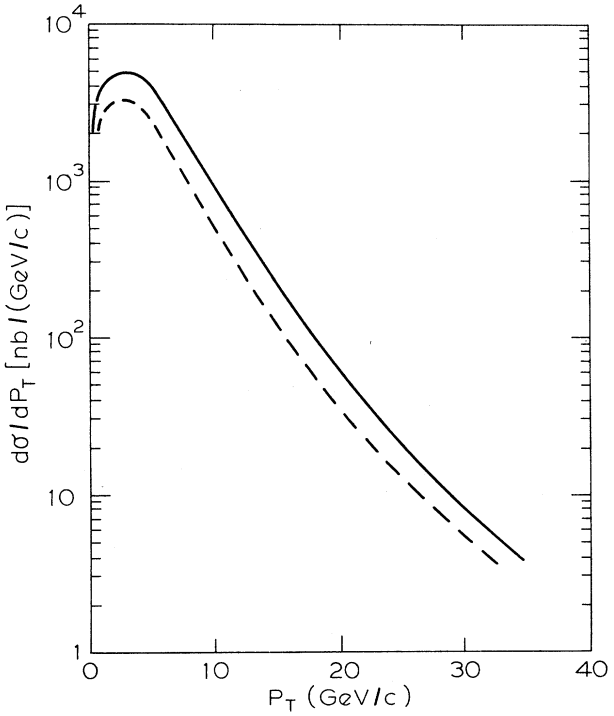

FIG. 12. $d\sigma/dp_T$ for b-quark production ($m_b = 5.0$ GeV/c^2) at $\sqrt{S} = 1.8$ TeV. Dashed line: $O(\alpha_s^2)$ cross section; solid line: sum of the $O(\alpha_s^2)$ cross section and the $O(\alpha_s^3)$ correction.

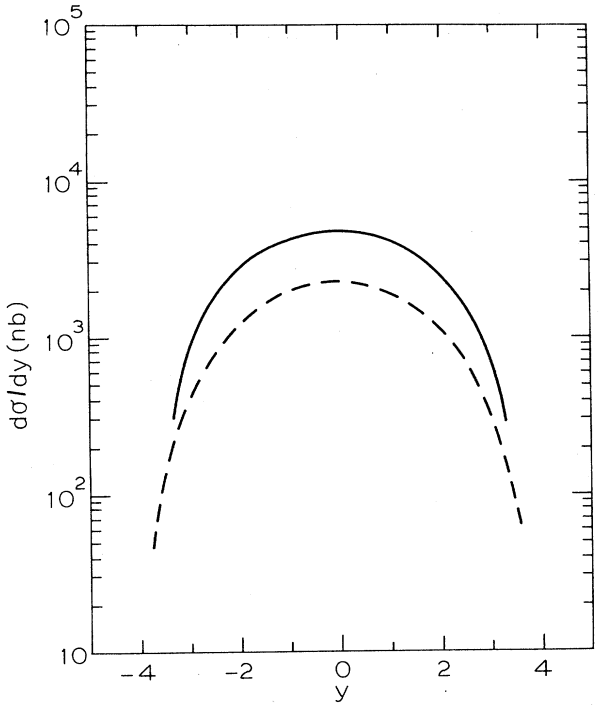

FIG. 14. $d\sigma/dy$ for b-quark production ($m_b = 5.0$ GeV/c^2) at $\sqrt{S} = 0.63$ TeV. Dashed line: $O(\alpha_s^2)$ cross section; solid line: sum of the $O(\alpha_s^2)$ cross section and the $O(\alpha_s^3)$ correction.

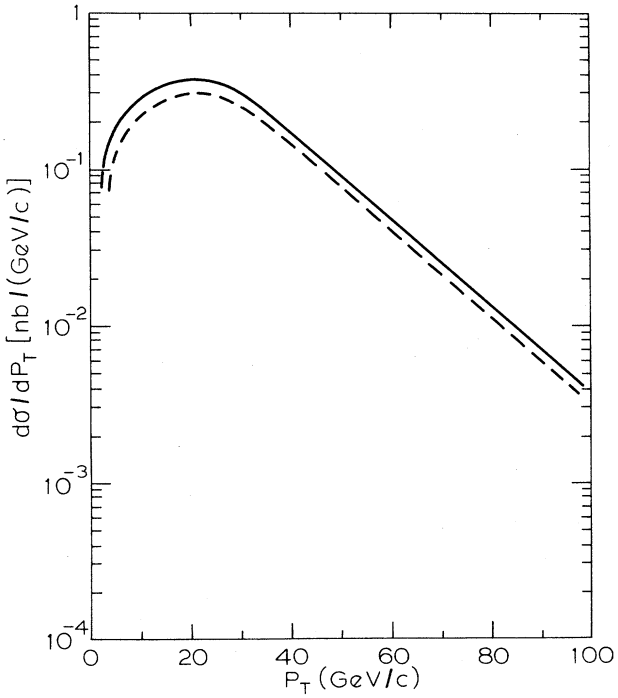

FIG. 13. $d\sigma/dp_T$ for t-quark production ($m_t = 40.0$ GeV/c^2) at $\sqrt{S} = 1.8$ TeV. Dashed line: $O(\alpha_s^2)$ cross section; solid line: sum of the $O(\alpha_s^2)$ cross section and the $O(\alpha_s^3)$ correction.

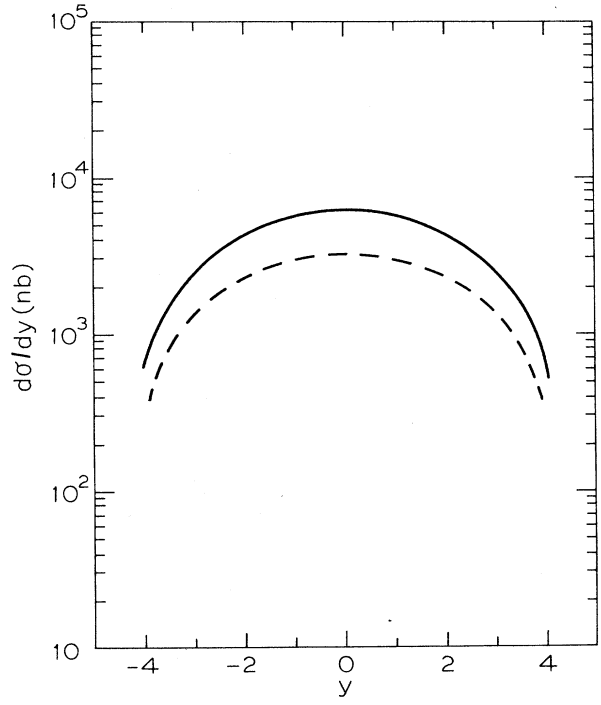

FIG. 15. $d\sigma/dy$ for b-quark production ($m_b = 5.0$ GeV/c^2) production at $\sqrt{S} = 1.8$ TeV. Dashed line: $O(\alpha_s^2)$ cross section; solid line: sum of the $O(\alpha_s^2)$ cross section and the $O(\alpha_s^3)$ correction.

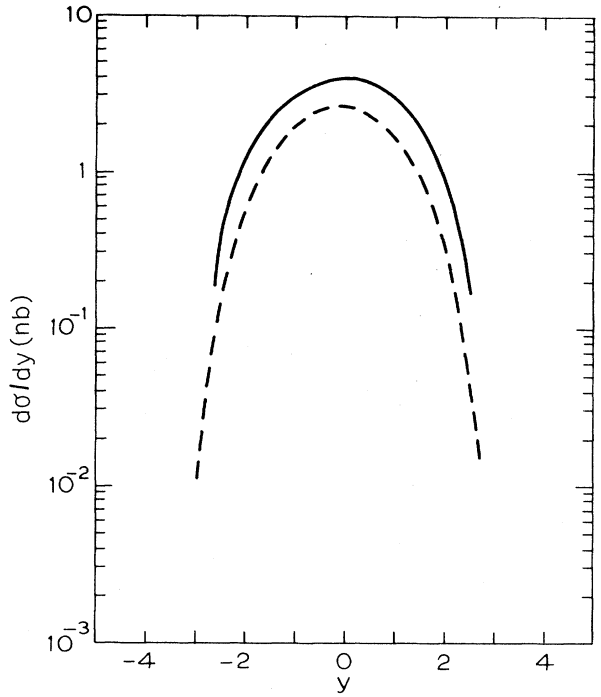

FIG. 16. $d\sigma/dy$ for t-quark production ($m_t = 40$ GeV/c^2) at $\sqrt{S} = 1.8$ TeV. Dashed line: $O(\alpha_s^2)$ cross section; solid line: sum of the $O(\alpha_s^2)$ cross section and the $O(\alpha_s^3)$ correction.

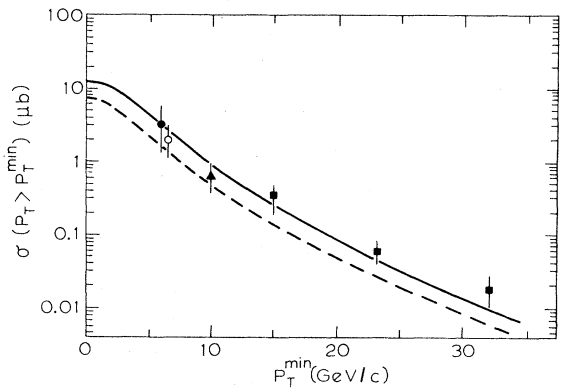

FIG. 17. The inclusive bottom cross section in $p\bar{p}$ collisions at $\sqrt{S} = 0.63$ TeV for $p_T(b) > p_T^{\min}$ and $|y(b)| < 1.5$ as a function of $p_T^{\min}$. The dashed curve is the theoretical prediction from the $O(\alpha_s^2)$ cross section and the solid line stands for the sum of the $O(\alpha_s^2)$ and the $O(\alpha_s^3)$ contributions computed in this paper.

cut $|y| < 1.5$. Since this is an inclusive b or $\bar{b}$ production cross section we have to multiply the total cross section values in Table III by a factor of 2. We have added the appropriate cuts to our computer programs to generate this $p_T > p_T^{\min}$ distribution. Figure 17 shows our results superimposed on the experimental data. Since the Born production cross section is too low, there is now direct evidence for the large QCD correction discussed in this paper. A more detailed theoretical analysis of the corrections to the p_T distribution will be presented in due course.

ACKNOWLEDGMENTS

We are indebted to Dr. Z. Kunszt for many discussions during the first stage of this project. The Stichting voor Fundamenteel Onderzoek der Materie supported the work of W. Beenakker. W. L. van Neerven would like to thank the Eidgenossische Technische Hochschule in Zürich and The Institute for Theoretical Physics in Stony Brook for their support where a part of this research has been carried out. The work of J. Smith was supported in part under NSF Grant No. 86-1108E and he would like to thank the Sektie Hoge-Energiefysica, Nationaal Instituut voor Kernfysica en Hoge-Energiefysica in Amsterdam for their hospitality while the paper was completed.

APPENDIX A

In this appendix we will list all scalar Feynman integrals which emerge from the Passarino-Veltman reduction technique applied to the graphs in Fig. 2. The notations for the one-, two-, three-, and four-point functions have been taken over from Ref. 23. Furthermore, we have

$$C_\epsilon = \frac{1}{16\pi^2} e^{\epsilon/2(\gamma_E - \ln 4\pi)} \left[\frac{m^2}{\mu^2}\right]^{\epsilon/2},$$
$$x = \frac{1-\sqrt{1-4m^2/s}}{1+\sqrt{1-4m^2/s}}, \tag{A1}$$
$$\zeta(2) = \frac{\pi^2}{6}.$$

The expressions for the scalar integrals are already analytically continued into the physical region. Only the real parts of the integrals are given. This is because any imaginary part will disappear when the first-order correction, containing these integrals, is contracted with the Born matrix element.

The one-loop four-point function is defined by

$$D(q_1,q_2,q_3,q_4,m_1,m_2,m_3,m_4) = \mu^{-\epsilon}\int \frac{d^n q}{(2\pi)^n} \frac{1}{(q^2-m_1^2)[(q+q_1)^2-m_2^2][(q+q_1+q_2)^2-m_3^2][(q+q_1+q_2+q_3)^2-m_4^2]}, \tag{A2}$$

where m_i represent the internal masses and the external outgoing momenta q_i satisfy the relation $\sum_{i=1}^4 q_i = 0$.

There are three different types of four-point functions. They are given by

$$D(p_1,-k_1,-k_2,p_2,0,m,m,m)=iC_\epsilon\frac{1}{st_1}\frac{1}{\sqrt{1-4m^2/s}}\times\left[-\frac{2}{\epsilon}\ln x-2\ln x\ln(1-x)+2\ln x\ln(1+x)-2\ln x\ln\frac{-t_1}{m^2}-2\mathrm{Li}_2(x)+2\mathrm{Li}_2(-x)-3\zeta(2)\right], \tag{A3}$$

$$D(-k_1,p_1,p_2,-k_2,0,0,m,0)=iC_\epsilon\frac{1}{st_1}\left[\frac{8}{\epsilon^2}+\frac{2}{\epsilon}\left[2\ln\frac{-t_1}{m^2}+\ln\frac{s}{m^2}\right]+2\ln\frac{s}{m^2}\ln\frac{-t_1}{m^2}-4\zeta(2)\right], \tag{A4}$$

$$D(-k_1,p_1,-k_2,p_2,0,0,m,m)=iC_\epsilon\frac{1}{t_1u_1}\left[\frac{4}{\epsilon^2}+\frac{2}{\epsilon}\left[\ln\frac{-t_1}{m^2}+\ln\frac{-u_1}{m^2}\right]+2\ln\frac{-t_1}{m^2}\ln\frac{-u_1}{m^2}-\frac{7}{2}\zeta(2)\right]. \tag{A5}$$

The other D functions can be obtained by interchanging $k_1\leftrightarrow k_2$ or $t_1\leftrightarrow u_1$.

The one-loop three-point function is defined by

$$C(q_1,q_2,q_3,m_1,m_2,m_3)=\mu^{-\epsilon}\int\frac{d^nq}{(2\pi)^n}\frac{1}{(q^2-m_1^2)[(q+q_1)^2-m_2^2][(q+q_1+q_2)^2-m_3^2]}. \tag{A6}$$

There are six different types of three-point functions which are listed below:

$$C(p_1,p_2,-k_1-k_2,0,m,0)=iC_\epsilon\frac{1}{s\sqrt{1-4m^2/s}}[2\mathrm{Li}_2(-x)+\tfrac{1}{2}\ln^2x+\zeta(2)], \tag{A7}$$

$$C(p_1,-k_1,p_2-k_2,0,m,m)=iC_\epsilon\frac{1}{t_1}[\zeta(2)-\mathrm{Li}_2(t/m^2)], \tag{A8}$$

$$C(-k_1,p_1,p_2-k_2,0,0,m)=iC_\epsilon\frac{1}{t_1}\left[\frac{2}{\epsilon^2}+\frac{2}{\epsilon}\ln\frac{-t_1}{m^2}+\ln^2\frac{-t_1}{m^2}+\mathrm{Li}_2\left[\frac{t}{m^2}\right]+\frac{1}{4}\zeta(2)\right], \tag{A9}$$

$$C(-k_1,-k_2,p_1+p_2,0,0,0)=iC_\epsilon\frac{1}{s}\left[\frac{4}{\epsilon^2}+\frac{2}{\epsilon}\ln\frac{s}{m^2}+\frac{1}{2}\ln^2\frac{s}{m^2}-\frac{7}{2}\zeta(2)\right], \tag{A10}$$

$$C(-k_1,-k_2,p_1+p_2,m,m,m)=iC_\epsilon\frac{1}{s}[\tfrac{1}{2}\ln^2x-3\zeta(2)], \tag{A11}$$

$$C(p_2,p_1,-k_1-k_2,m,0,m)=iC_\epsilon\frac{1}{s\sqrt{1-4m^2/s}}\left[-\frac{2}{\epsilon}\ln x-2\ln x\ln(1-x)-2\,\mathrm{Li}_2(x)+\frac{1}{2}\ln^2x-4\zeta(2)\right]. \tag{A12}$$

The other C functions can be obtained by interchanging $k_1\leftrightarrow k_2$ or $t_1\leftrightarrow u_1$.

The one-loop two-point function is defined by

$$B(q_1,m_1,m_2)=\mu^{-\epsilon}\int\frac{d^nq}{(2\pi)^n}\frac{1}{(q^2-m_1^2)[(q+q_1)^2-m_2^2]}. \tag{A13}$$

There are five different types of two-point functions:

$$B(p_1-k_1,0,m)=iC_\epsilon\left[-\frac{2}{\epsilon}+2-\frac{t_1}{t}\ln\frac{-t_1}{m^2}\right], \tag{A14}$$

$$B(p_1+p_2,m,m)=iC_\epsilon\left[-\frac{2}{\epsilon}+2+\sqrt{1-4m^2/s}\,\ln x\right], \tag{A15}$$

$$B(p_1,0,m)=iC_\epsilon\left[-\frac{2}{\epsilon}+2\right], \tag{A16}$$

$$B(k_1,m,m)=iC_\epsilon\left[-\frac{2}{\epsilon}\right], \tag{A17}$$

$$B(p_1+p_2,0,0)=iC_\epsilon\left[-\frac{2}{\epsilon}+2-\ln\frac{s}{m^2}\right]. \tag{A18}$$

The other B functions can be obtained by interchanging $k_1\leftrightarrow k_2$ or $t_1\leftrightarrow u_1$.

The one-loop one-point function is defined by

$$A(m)=\mu^{-\epsilon}\int\frac{d^nq}{(2\pi)^n}\frac{1}{q^2-m^2}. \tag{A19}$$

There is only one type:

$$A(m)=iC_\epsilon m^2\left[-\frac{2}{\epsilon}+1\right]. \tag{A20}$$

APPENDIX B

In this appendix we outline the kinematics for the reactions discussed in the text. The two-to-three-body process in (4.1) is described in the c.m. frame of the recoiling gluon and quark (antiquark).[26,35] In n dimensions the momenta are given by

$$k_1=(\omega_1,0,\ldots,0,|\mathbf{p}|\sin\psi,|\mathbf{p}|\cos\psi-\omega_2), \tag{B1}$$

$$k_2=(\omega_2,0,\ldots,0,0,\omega_2), \tag{B2}$$

$$k_3=(\omega_3,0,\ldots,0,\omega_3\sin\theta_1\sin\theta_2,\omega_3\sin\theta_1\cos\theta_2,\omega_3\cos\theta_1), \tag{B3}$$

$$p_1=(E_1,0,\ldots,0,-\omega_3\sin\theta_1\sin\theta_2,-\omega_3\sin\theta_1\cos\theta_2,-\omega_3\cos\theta_1), \tag{B4}$$

$$p_2=(E_2,0,\ldots,0,0,|\mathbf{p}|\sin\psi,|\mathbf{p}|\cos\psi), \tag{B5}$$

where the dots in (B1)–(B5) stand for $n-3$ equal and opposite angular components.

From four-momentum conservation and the on-mass-shell constraints one can derive the identities

$$\begin{aligned}
&\omega_1=\frac{s+u_1}{2\sqrt{s_4+m^2}},\quad \omega_2=\frac{s+t_1}{2\sqrt{s_4+m^2}},\quad \omega_3=\frac{s_4}{2\sqrt{s_4+m^2}},\\
&E_1=\frac{s_4+2m^2}{2\sqrt{s_4+m^2}},\quad E_2=-\frac{t_1+u_1+2m^2}{2\sqrt{s_4+m^2}},\\
&|\mathbf{p}|=\frac{\sqrt{(t_1+u_1)^2-4m^2s}}{2\sqrt{s_4+m^2}},\\
&\cos\psi=\frac{t_1s_4-s(u_1+2m^2)}{(s+t_1)\sqrt{(t_1+u_1)^2-4m^2s}},
\end{aligned} \tag{B6}$$

where s, t_1, u_1, and s_4 are defined in (4.2). Furthermore we have the relation

$$s+t_1+u_1=s_4. \tag{B7}$$

The cross section is given by

$$\sigma=K(\tfrac{1}{2})^2\frac{\mu^{-2\epsilon}}{2s}\int\frac{d^np_2}{(2\pi)^{n-1}}\int\frac{d^nk_3}{(2\pi)^{n-1}}\int\frac{d^np_1}{(2\pi)^{n-1}}\delta^+(p_2^2-m^2)\delta^+(k_3^2)\times\delta^+(p_1^2-m^2)(2\pi)^n\delta^n(k_1+k_2-k_3-p_1-p_2)|M^R|^2, \tag{B8}$$

where M^R is the matrix element of the process given in (4.1) and $\epsilon=n-4$. The factor $(1/2)^2$ is from the average over the initial gluon helicities, and K is the color-average factor defined in (2.12) and (2.13). The integral can be rewritten as

$$\sigma=K(\tfrac{1}{2})^2\frac{1}{2s}\frac{\mu^{-2\epsilon}}{(2\pi)^{2n-3}}\int d^np_2d^np\,\delta^+(p_2^2-m^2)\delta^n(k_1+k_2-p_2-p)\times\int d^nk_3d^np_1\delta^+(k_3^2)\delta^+(p_1^2-m^2)\delta^n(p-k_3-p_1)|M^R|^2. \tag{B9}$$

The second factor in (B9) is the standard two-body phase-space integral. Its evaluation in the c.m. frame of the gluon and the quark yields

$$\int d^nk_3d^np_1\delta^+(k_3^2)\delta^+(p_1^2-m^2)\delta^n(p-k_3-p_1)|M^R|^2=\tfrac{1}{4}\pi^{n/2-2}\frac{\Gamma(n/2-1)}{\Gamma(n-3)}\frac{(p^2-m^2)^{n-3}}{(p^2)^{n/2-1}}\int_0^\pi d\theta_1\sin^{n-3}\theta_1\int_0^\pi d\theta_2\sin^{n-4}\theta_2|M^R|^2. \tag{B10}$$

After integration over the n-dimensional vector p, the cross section can be expressed in terms of variables chosen in the c.m. frame of the antiquark and the quark-gluon pair. In this frame we have the parametrization

$$k_1=\tfrac{1}{2}\sqrt{s}\,(1,0,\ldots,0,1),\quad k_2=\tfrac{1}{2}\sqrt{s}\,(1,0,\ldots,0,-1),\quad p_2=(E_2,0,\ldots,0,|\mathbf{p}|\sin\chi,|\mathbf{p}|\cos\chi). \tag{B11}$$

Hence the cross section is

$$\sigma=K(\tfrac{1}{2})^2\frac{1}{s}\frac{S_\epsilon^2\mu^{-2\epsilon}}{\Gamma(n-3)}\int dE_2(E_2^2-m^2)^{n/2-3/2}\int_0^\pi d\chi\sin^{n-3}\chi\frac{s_4^{n-3}}{(s_4+m^2)^{n/2-1}}\int_0^\pi d\theta_1\sin^{n-3}\theta_1\int_0^\pi d\theta_2\sin^{n-4}\theta_2|M^R|^2, \tag{B12}$$

where we have integrated over all angles of the gluon momentum which do not appear in $|M^R|^2$. After changing the integration variables E_2 and χ to t_1 and u_1, using

$$E_2=-\frac{t_1+u_1}{2\sqrt{s}},\quad \cos\chi=\frac{u_1-t_1}{\sqrt{(t_1+u_1)^2-4sm^2}}\ , \tag{B13}$$

we find

$$s^2\frac{d^2\sigma}{dt_1du_1}=K(\tfrac{1}{2})^3\frac{S_\epsilon^2\mu^{-\epsilon}}{\Gamma(n-3)}\left[\frac{t_1u_1-sm^2}{s\mu^2}\right]^{n/2-2}\frac{s_4^{n-3}}{(s_4+m^2)^{n/2-1}}\int_0^\pi d\theta_1\sin^{n-3}\theta_1\int_0^\pi d\theta_2\sin^{n-4}\theta_2|M^R|^2\ , \tag{B14}$$

which is the formula used in Sec. IV.

APPENDIX C

Here we give the angular integrals of the terms $(s')^k(s'')^l$ which arise from the partial fractioning of the square of matrix element $|M^R|^2$ in (4.3). The general expression for the angular integral is given in (4.9). The specific four-dimensional integrals for $a^2\neq b^2$ and $A^2\neq B^2+C^2$ are listed first:[25]

$$I_4^{(0,0)}=2\pi\ , \tag{C1}$$

$$I_4^{(-1,0)}=2\pi a\ , \tag{C2}$$

$$I_4^{(0,-1)}=2\pi A\ , \tag{C3}$$

$$I_4^{(1,0)}=\frac{\pi}{b}\ln\frac{a+b}{a-b}\ , \tag{C4}$$

$$I_4^{(0,1)}=\frac{\pi}{\sqrt{B^2+C^2}}\ln\left[\frac{A+\sqrt{B^2+C^2}}{A-\sqrt{B^2+C^2}}\right], \tag{C5}$$

$$I_4^{(1,1)}=\frac{\pi}{\sqrt{X}}\ln\left[\frac{aA-bB+\sqrt{X}}{aA-bB-\sqrt{X}}\right], \tag{C6}$$

$$I_4^{(1,2)}=\pi\left[\frac{2a(B^2+C^2)-2bAB}{(A^2-B^2-C^2)X}+\frac{b(bA-aB)}{X^{3/2}}\ln\left[\frac{aA-bB+\sqrt{X}}{aA-bB-\sqrt{X}}\right]\right], \tag{C7}$$

$$I_4^{(2,1)}=\pi\left[\frac{2b(bA-aB)}{(a^2-b^2)X}+\frac{a(B^2+C^2)-bAB}{X^{3/2}}\ln\left[\frac{aA-bB+\sqrt{X}}{aA-bB-\sqrt{X}}\right]\right], \tag{C8}$$

$$I_4^{(2,2)}=\pi\left[\frac{2b^2}{(a^2-b^2)X}+\frac{2(B^2+C^2)}{(A^2-B^2-C^2)X}-\frac{6b^2C^2}{X^2}+\left[\frac{bB}{X^{3/2}}+\frac{3b(bA-aB)[a(B^2+C^2)-bAB]}{X^{5/2}}\right]\ln\left[\frac{aA-bB+\sqrt{X}}{aA-bB-\sqrt{X}}\right]\right], \tag{C9}$$

with $X=(aA-bB)^2-(A^2-B^2-C^2)(a^2-b^2)$,

$$I_4^{(-1,-1)}=2\pi(aA+\tfrac{1}{3}bB)\ , \tag{C10}$$

$$I_4^{(-1,1)}=\pi\left[\frac{2bB}{B^2+C^2}+\frac{a(B^2+C^2)-bAB}{(B^2+C^2)^{3/2}}\times\ln\left[\frac{A+\sqrt{B^2+C^2}}{A-\sqrt{B^2+C^2}}\right]\right], \tag{C11}$$

$$I_4^{(0,2)}=2\pi\frac{1}{A^2-B^2-C^2}\ , \tag{C12}$$

$$I_4^{(-2,0)}=2\pi(a^2+\tfrac{1}{3}b^2)\ , \tag{C13}$$

$$I_4^{(0,-2)}=2\pi[A^2+\tfrac{1}{3}(B^2+C^2)]\ , \tag{C14}$$

$$I_4^{(-2,1)}=\pi\left[\frac{4abB}{B^2+C^2}+\frac{b^2A(C^2-2B^2)}{(B^2+C^2)^2}+\left[\frac{[a(B^2+C^2)-bAB]^2}{(B^2+C^2)^{5/2}}-\frac{b^2C^2(A^2-B^2-C^2)}{2(B^2+C^2)^{5/2}}\right]\times\ln\left[\frac{A+\sqrt{B^2+C^2}}{A-\sqrt{B^2+C^2}}\right]\right], \tag{C15}$$

$$I_4^{(-1,2)}=\pi\left[\frac{2[a(B^2+C^2)-bAB]}{(B^2+C^2)(A^2-B^2-C^2)}+\frac{bB}{(B^2+C^2)^{3/2}}\ln\left[\frac{A+\sqrt{B^2+C^2}}{A-\sqrt{B^2+C^2}}\right]\right], \tag{C16}$$

$$I_4^{(-2,2)}=\pi\left[\frac{2b^2(B^2-C^2)}{(B^2+C^2)^2}+\frac{2[a(B^2+C^2)-bAB]^2}{(A^2-B^2-C^2)(B^2+C^2)^2}+\left[\frac{2bB[a(B^2+C^2)-bAB]}{(B^2+C^2)^{5/2}}+\frac{b^2AC^2}{(B^2+C^2)^{5/2}}\right]\times\ln\left[\frac{A+\sqrt{B^2+C^2}}{A-\sqrt{B^2+C^2}}\right]\right], \tag{C17}$$

$$I_4^{(2,-2)}=\pi\left[\frac{2(B^2-C^2)}{b^2}+\frac{2(bA-aB)^2}{b^2(a^2-b^2)}+\frac{aC^2+2B(bA-aB)}{b^3}\ln\left[\frac{a+b}{a-b}\right]\right], \quad \text{(C18)}$$

In n dimensions[24,25] we need the following integrals, which we classify into groups where $b=-a$, $A^2=B^2+C^2$, or $b=-a$, $A^2\neq B^2+C^2$, or $a^2\neq b^2$, $A^2=B^2+C^2$, respectively.

Group 1, $b=-a$ and $A^2=B^2+C^2$:

$$\hat{I}_n^{(1,0)}=2\pi\frac{1}{a}\frac{1}{n-4}, \quad \text{(C19)}$$

$$\hat{I}_n^{(1,1)}=2\pi\frac{1}{aA}\frac{1}{n-4}F_{1,2}\left[1,1,\tfrac{1}{2}n-1,\frac{A-B}{2A}\right]$$
$$=2\pi\frac{1}{aA}\frac{1}{n-4}\left[\frac{A+B}{2A}\right]^{n/2-3}\left[1+\tfrac{1}{4}(n-4)^2\mathrm{Li}_2\left[\frac{A-B}{2A}\right]+O((n-4)^3)\right], \quad \text{(C20)}$$

$$\hat{I}_n^{(-1,1)}=2\pi\frac{a}{A}\frac{n-2}{(n-4)(n-3)}F_{1,2}\left[-1,1,\frac{1}{2}n-1,\frac{A-B}{2A}\right]=\pi\frac{a(A+B)}{A^2}\left[\frac{2}{n-4}-\frac{2B}{A+B}+O(n-4)\right], \quad \text{(C21)}$$

$$\hat{I}_n^{(-2,1)}=2\pi\frac{a^2}{A}\frac{n}{(n-4)(n-3)}F_{1,2}\left[-2,1,\frac{1}{2}n-1,\frac{A-B}{2A}\right]=\pi\frac{a^2(A+B)^2}{A^3}\left[\frac{2}{n-4}+\frac{A^2-4AB-3B^2}{(A+B)^2}+O(n-4)\right]. \quad \text{(C22)}$$

Group 2, $b=-a$ and $A^2\neq B^2+C^2$:

$$\bar{I}_n^{(1,-1)}=\pi\frac{A+B}{a}\left[\frac{2}{n-4}-\frac{2B}{A+B}+O(n-4)\right], \quad \text{(C23)}$$

$$\bar{I}_n^{(1,-2)}=\pi\frac{(A+B)^2}{a}\left[\frac{2}{n-4}+\frac{C^2-4AB-2B^2}{(A+B)^2}+O(n-4)\right], \quad \text{(C24)}$$

$$\bar{I}_n^{(1,1)}=\pi\frac{1}{a(A+B)}\left\{\frac{2}{n-4}+\ln\left[\frac{(A+B)^2}{A^2-B^2-C^2}\right]+\frac{n-4}{2}\left[\ln^2\left[\frac{A-\sqrt{B^2+C^2}}{A+B}\right]-\frac{1}{2}\ln^2\left[\frac{A+\sqrt{B^2+C^2}}{A-\sqrt{B^2+C^2}}\right]+2\,\mathrm{Li}_2\left[-\frac{B+\sqrt{B^2+C^2}}{A-\sqrt{B^2+C^2}}\right]-2\,\mathrm{Li}_2\left[\frac{B-\sqrt{B^2+C^2}}{A+B}\right]\right]+O((n-4)^2)\right\}, \quad \text{(C25)}$$

$$\bar{I}_n^{(1,2)}=\pi\frac{1}{a(A+B)^2}\left\{\frac{2}{n-4}+\ln\left[\frac{(A+B)^2}{A^2-B^2-C^2}\right]+\frac{2(B^2+C^2+AB)}{A^2-B^2-C^2}+\frac{n-4}{2}\left[\ln^2\left[\frac{A-\sqrt{B^2+C^2}}{A+B}\right]-\frac{1}{2}\ln^2\left[\frac{A+\sqrt{B^2+C^2}}{A-\sqrt{B^2+C^2}}\right]+2\,\mathrm{Li}_2\left[-\frac{B+\sqrt{B^2+C^2}}{A-\sqrt{B^2+C^2}}\right]-2\,\mathrm{Li}_2\left[\frac{B-\sqrt{B^2+C^2}}{A+B}\right]-2\frac{(A+B)\sqrt{B^2+C^2}}{A^2-B^2-C^2}\ln\left[\frac{A+\sqrt{B^2+C^2}}{A-\sqrt{B^2+C^2}}\right]-2\ln\left[\frac{(A+B)^2}{A^2-B^2-C^2}\right]\right]+O((n-4)^2)\right\}, \quad \text{(C26)}$$

$$\bar{I}_n^{(2,0)}=-\pi\frac{1}{a^2}+O(n-4) \quad \text{(C27)}$$

$$\bar{I}_n^{(2,1)}=\pi\frac{1}{a^2(A+B)}\left\{\frac{B^2+AB+C^2}{(A+B)^2}\left[\frac{2}{n-4}+\ln\left[\frac{(A+B)^2}{A^2-B^2-C^2}\right]\right]-\frac{2C^2}{(A+B)^2}-1+O(n-4)\right\}, \tag{C28}$$

$$\bar{I}_n^{(2,2)}=\pi\frac{1}{a^2(A+B)^2}\left[\left[\frac{3C^2}{(A+B)^2}+\frac{2B}{A+B}\right]\left[\frac{2}{n-4}+\ln\left[\frac{(A+B)^2}{A^2-B^2-C^2}\right]\right]-\frac{8C^2}{(A+B)^2}+\frac{2(B^2+C^2)}{A^2-B^2-C^2}-1+O(n-4)\right]. \tag{C29}$$

Group 3, $a^2\neq b^2$ and $A^2=B^2+C^2$:

$$\tilde{I}_n^{(1,1)}=\pi\frac{1}{aA-bB}\left[\frac{2}{n-4}+\ln\frac{(aA-bB)^2}{(a^2-b^2)A^2}+O(n-4)\right], \tag{C30}$$

$$\tilde{I}_n^{(2,1)}=\pi\frac{A}{(aA-bB)^2}\left[\frac{2}{n-4}+\ln\frac{(aA-bB)^2}{(a^2-b^2)A^2}+\frac{2b(bA-aB)}{A(a^2-b^2)}+O(n-4)\right]. \tag{C31}$$

From the partial fractioning of the two- to three-body matrix element in (4.5) we obtain 32 independent integrals. However, since the parametrization of the incoming momenta can be interchanged using (4.7) there exists a $t_1\leftrightarrow u_1$ symmetry. This implies that the number of independent functions is reduced. It appears that there are only 19 independent types. These 19 integrals belong to 7 different classes which are characterized by the dependence of the functions a, b, A, B, and C on the variables s, t_1, u_1, m^2. Note that many integrals can be obtained from the other results by interchanging t_1 and u_1.

APPENDIX D

In this appendix we give the results for the virtual plus soft terms in (6.19). The first term is

$$\begin{aligned}
F_0^{V+S}(t,u,t_1,u_1)=4B_{\rm QED}&\left\{2(t_1^2+u_1^2)s^{-2}\ln^2\delta+\left[(t_1^2+u_1^2)s^{-2}\left[-1+\ln\frac{(1+x)^2}{x}\right]-4t_1^2s^{-2}\ln\left[\frac{-t_1}{m^2}\right]\right]\ln\delta\right\}\\
&+2-[4(s+2m^2)s^{-1}+2(t-u)^2s^{-2}]\zeta(2)-m^2(t-u)^4s_1^{-1}s^{-2}t^{-1}u^{-1}\\
&+(t-u)^2[s^{-1}s_1^{-1}-\tfrac{3}{16}ss_1^{-1}t^{-1}u^{-1}+s^{-2}-\tfrac{11}{16}t^{-1}u^{-1}+\tfrac{3}{4}m^2s^{-1}t^{-1}u^{-1}+m^4s^{-2}t^{-1}u^{-1}]\\
&+ss_1^{-1}-\tfrac{3}{16}s^3s_1^{-1}t^{-1}u^{-1}-\tfrac{63}{16}s^2t^{-1}u^{-1}+\tfrac{80}{3}m^2s^{-1}+\tfrac{19}{4}sm^2t^{-1}u^{-1}+8m^4t^{-1}u^{-1}-8m^6s^{-1}t^{-1}u^{-1}\\
&-\{4(s+2m^2)+24sm^4s_1^{-2}+(t-u)^2(\tfrac{3}{2}ss_1^{-2}+\tfrac{5}{2}s_1^{-1}+3s^{-1})\\
&\quad -s(s^2+2sm^2-4m^4+6s^2m^4s_1^{-2})t_1^{-1}u_1^{-1}\}\zeta(2)\bar{s}^{-1}\\
&+[\tfrac{1}{2}s(17s-8m^2)u^{-1}+4sm^2t^{-1}-\tfrac{3}{32}s^4s_1^{-1}t^{-1}u^{-1}]t_1^{-1}\\
&+\{\tfrac{3}{64}s^4t^{-1}u^{-1}+\tfrac{3}{16}s^3m^2t^{-1}u^{-1}-\tfrac{1}{4}s^3s_1^{-1}-s^2[\tfrac{11}{2}-\zeta(2)]\\
&\quad -sm^2[\tfrac{32}{3}-4\zeta(2)]-m^4[16-16\zeta(2)]\}t_1^{-1}u_1^{-1}\\
&+2s^4t_1^{-2}u_1^{-2}+4s^2(s-m^2)t_1^{-2}u^{-1}+8s^2m^4[1-\zeta(2)]t_1^{-2}u_1^{-2}\\
&+[-11-5(t-u)s^{-1}-8m^2s^{-1}+2(s^2-5sm^2-3m^4)s^{-1}t^{-1}\\
&\quad -2m^4(s+m^2)s^{-1}t^{-2}-8(s+2m^2)t_1^{-1}-32m^4t_1^{-2}]\ln\left[\frac{-t_1}{m^2}\right]\\
&+\{4(s-2m^2)s^{-1}+5ss_1^{-1}+3s^2s_1^{-2}+(t-u)^2(3s_1^{-2}+4s^{-1}s_1^{-1}-2s^{-2})\\
&\quad -\tfrac{1}{4}s[2(s-4m^2)+3s^3s_1^{-2}+5s^2s_1^{-1}]t_1^{-1}u_1^{-1}\}\ln\frac{(1+x)^2}{x}\\
&-[2+2(t-u)^2s^{-2}-8(t-u)s^{-1}-4(s+4m^2)t_1^{-1}\\
&\quad -2(s^2+4sm^2+8m^4)t_1^{-1}u_1^{-1}+8s^2m^4t_1^{-2}u_1^{-2}]\ln\left[\frac{-t_1}{m^2}\right]\ln\left[\frac{t_1}{u_1}\right]
\end{aligned}$$

$$
\begin{aligned}
&+[4u_1(s+4m^2)s^{-1}t_1^{-1}-8(t-u)s^{-1}] \\
&\quad\times\left[\mathrm{Li}_2\left[1-\frac{t_1}{xu_1}\right]-\mathrm{Li}_2\left[\frac{t}{m^2}\right]-\ln\left[\frac{-t_1}{m^2}\right]\ln\left[\frac{-u_1}{m^2}\right]-\ln x\,\ln\left[\frac{-t_1}{m^2}\right]\right] \\
&-[8(s+2m^2)+48sm^4s_1^{-2}+(t-u)^2(3ss_1^{-2}+5s_1^{-1}+6s^{-1}) \\
&\quad-2s(s^2+2sm^2-4m^4+6s^2m^4s_1^{-2})t_1^{-1}u_1^{-1}][\mathrm{Li}_2(-x)+\tfrac{1}{4}\ln^2 x]\bar{s}^{-1} \\
&+2(s+4m^2)(2-s^2t_1^{-1}u_1^{-1})s^{-1}\ln(1+x)\ln\frac{1+x}{x} \\
&+[4(s+3m^2)s^{-1}+(t-u)^2s^{-2}-\tfrac{1}{2}(3s^2+12sm^2+16m^4)t_1^{-1}u_1^{-1}+4s^2m^4t_1^{-2}u_1^{-2}]\ln^2 x \\
&+[2(3s+8m^2)s^{-1}+2(t-u)^2s^{-2}-2(s^2+4sm^2+8m^4)t_1^{-1}u_1^{-1}+8s^2m^4t_1^{-2}u_1^{-2}] \\
&\quad\times\left[\mathrm{Li}_2\left[1-\frac{t_1u_1}{sm^2}\right]+2\,\mathrm{Li}_2\left[1-\frac{t_1}{xu_1}\right]-2\ln x\,\ln\left[\frac{-t_1}{m^2}\right]+(s-2m^2)\bar{s}^{-1}\ln x\right] \\
&+[8(s+2m^2)s^{-1}+4(t-u)^2s^{-2}+4(s+4m^2)t_1^{-1}+32m^4t_1^{-2}]\left[2\ln(1+x)\ln\left[\frac{-t_1}{m^2}\right]-\mathrm{Li}_2\left[1-\frac{t_1}{xu_1}\right]\right],
\end{aligned}
\tag{D1}
$$

where x is defined in (5.10). Further we denote

$$s_1=4m^2-s,\quad \bar{s}=s\sqrt{1-4m^2/s}\ .$$

B_{QED} is defined in (2.7) and $\delta=\Delta/m^2$, where Δ is defined in (4.13).

The second term is given by

$$
\begin{aligned}
&F_K^{V+S}(t,u,t_1,u_1) \\
&=-4B_{\mathrm{QED}}\{2\ln^2\delta-[(3t_1^2+3u_1^2+4t_1u_1)s^{-2}+(s-2m^2)(t_1^2+u_1^2)s^{-2}\bar{s}^{-1}\ln x]\ln\delta\}-2+(9+8m^2s^{-1})\zeta(2) \\
&\quad-(t-u)^2(s^{-2}+m^4s^{-2}t^{-1}u^{-1}+\tfrac{5}{4}m^2s^{-1}t^{-1}u^{-1}-\tfrac{19}{16}t^{-1}u^{-1}) \\
&\quad+\tfrac{1}{4}(t-u)^4s^{-2}t^{-1}u^{-1}+128m^8s^{-2}t^{-1}u^{-1}-190m^6s^{-1}t^{-1}u^{-1} \\
&\quad-\tfrac{1}{4}sm^2t^{-1}u^{-1}-\tfrac{297}{16}s^2t^{-1}u^{-1}+92m^4t^{-1}u^{-1}-26m^2s^{-1} \\
&\quad+\{(19s^2+8sm^2-112m^4)s^{-1}+6(t-u)^2s^{-1}-12m^2(t-u)^2s^{-2} \\
&\qquad-(s-2m^2)[(5s^2+20sm^2+32m^4)t_1^{-1}u_1^{-1}-16s^2m^4t_1^{-2}u_1^{-2}]\}\zeta(2)\bar{s}^{-1} \\
&\quad-12sm^2(s-m^2)t_1^{-2}u^{-1}-8s^4m^4\zeta(2)t_1^{-3}u_1^{-3}+2s^2m^2\{s-m^2[12-26\zeta(2)]\}t_1^{-2}u_1^{-2} \\
&\quad+[(-3s^3+6s^2m^2+84sm^4-64m^6)s^{-1}-3(s^2-2sm^2+20m^4)\zeta(2)+\tfrac{183}{64}s^4t^{-1}u^{-1}+\tfrac{3}{16}m^2tus^{-1}]t_1^{-1}u_1^{-1} \\
&\quad+[\tfrac{1}{16}(t+u)^3s^{-2}-\tfrac{13}{32}(t^3+u^3)s^{-2}+\tfrac{3}{32}(t^5+u^5)s^{-2}u^{-1}t^{-1} \\
&\qquad+\tfrac{1}{4}m^2(t^2+u^2)s^{-2}-\tfrac{93}{16}s^2t^{-1}+\tfrac{283}{16}s^2u^{-1}-\tfrac{1}{16}t^3s^{-1}u^{-1} \\
&\qquad-128m^8s^{-2}u^{-1}+264m^6s^{-1}u^{-1}-176m^4u^{-1}+8m^2su^{-1}]t_1^{-1} \\
&\quad+[20+2(t+7m^2)s^{-1}-(14s^2-74sm^2+2m^4)t^{-1}s^{-1}+2m^2(8s^2+7sm^2+m^4)s^{-1}t^{-2}-16m^2(s-6m^2)t_1^{-2} \\
&\qquad+32(s-m^2)t_1^{-1}+8m^2(2s^2-sm^2-2m^4)t^{-2}u_1^{-1}+8m^2(s^2-11sm^2+8m^4)t^{-1}t_1^{-1}u_1^{-1}]\ln\left[\frac{-t_1}{m^2}\right] \\
&\quad-[\tfrac{311}{20}s-64m^4s^{-1}-\tfrac{18}{5}t_1^3s^{-2}+\tfrac{73}{20}(t-u)^2s^{-1}-12m^2(t-u)^2s^{-2} \\
&\qquad-(6s^3+17s^2m^2-40sm^4-32m^6)t_1^{-1}u_1^{-1}+24s^2m^4(s-2m^2)t_1^{-2}u_1^{-2}]\bar{s}^{-1}\ln x \\
&\quad+16m^4(s^2t_1^{-1}u_1^{-1}-2)t_1^{-1}u_1^{-1}\ln^2\left[\frac{-t_1}{m^2}\right] \\
&\quad-(\{\tfrac{1}{2}(19s^2+8sm^2-112m^4)s^{-1} \\
&\qquad+(s-2m^2)[3(t-u)^2s^{-2}+8s^2m^4t_1^{-2}u_1^{-2}-\tfrac{1}{2}(5s^2+20sm^2+32m^4)t_1^{-1}u_1^{-1}]\}\bar{s}^{-1}
\end{aligned}
$$

$$
\begin{aligned}
&-\tfrac{1}{2}(3s^2+18sm^2+4m^4)t_1^{-1}u_1^{-1}+\tfrac{1}{2}(9s+8m^2)s^{-1}+8s^2m^4t_1^{-2}u_1^{-2})\ln^2 x \\
&-[2(s^2-4m^2s-16m^4)s^{-1}-2(t-u)-4(s-2m^2)(8m^4t_1^{-2}+(s+4m^2)t_1^{-1})]\bar{s}^{-1}\ln x\ln\left[\frac{-t_1}{m^2}\right] \\
&-[16-8(s+2m^2)^2t_1^{-1}u_1^{-1}+48s^2m^4t_1^{-2}u_1^{-2}]\ln\left[\frac{-t_1}{m^2}\right]\ln\left[\frac{-u_1}{m^2}\right] \\
&-[2(7s-8m^2)s^{-1}+2(t-u)s^{-1}+16sm^4t_1^{-3}-8m^4t_1^{-2} \\
&\quad +4(s+2m^2)(s-4m^2)s^{-1}t_1^{-1}-8(s^2+sm^2-3m^4)t_1^{-1}u_1^{-1}]\mathrm{Li}_2\left[\frac{t}{m^2}\right] \\
&+8(s-2m^2)[3+8m^2s^{-1}+(t-u)^2s^{-2}-(s^2+4sm^2+8m^4)t_1^{-1}u_1^{-1} \\
&\qquad +4s^2m^4t_1^{-2}u_1^{-2}][\ln x\ln(1-x)+\mathrm{Li}_2(x)]\bar{s}^{-1} \\
&+\{14s-96m^4s^{-1}+2(s-2m^2)[2(t-u)^2s^{-2}-s(s+4m^2)t_1^{-1}u_1^{-1}]\}[\ln x\ln(1+x)+\mathrm{Li}_2(-x)]\bar{s}^{-1}\,, \qquad \text{(D2)}
\end{aligned}
$$

with the same definitions as above.

The third term is given by[18]

$$
\begin{aligned}
&F_{\mathrm{QED}}^{V+S}(t,u,t_1,u_1) \\
&\quad=-4B_{\mathrm{QED}}[1+(s-2m^2)\bar{s}^{-1}\ln x]\ln\delta \\
&\quad+2\zeta(2)+2+3m^2(s-2m^2)t^{-1}u^{-1}-4m^2(s-2m^2)(5s-8m^2)s^{-2}t^{-1} \\
&\quad-[10s-24m^2-s(3s^2+10sm^2-24m^4)t_1^{-1}u_1^{-1}+16s^2m^4(s-2m^2)t_1^{-2}u_1^{-2}]\zeta(2)\bar{s}^{-1} \\
&\quad+[28sm^2+32m^4-(3s^2+8m^4)\zeta(2)]t_1^{-1}u_1^{-1}-8sm^2[4sm^2+8m^4+sm^2\zeta(2)]t_1^{-2}u_1^{-2} \\
&\quad-4s^2m^4[s^2-8sm^2-s^2\zeta(2)]t_1^{-3}u_1^{-3}-8m^4(s-8m^2)t_1^{-3} \\
&\quad+[2s+52m^2-72m^4s^{-1}+64m^6s^{-2}-(20sm^2-100m^4+136m^6s^{-1}-64m^8s^{-2})u^{-1}]t_1^{-1} \\
&\quad-4m^2[s-26m^2+16m^4s^{-1}-s(s-m^2)u^{-1}]t_1^{-2} \\
&\quad+[4s(1-sm^2t_1^{-1}u_1^{-1})+2(s-2m^2)(2-s(s+4m^2)t_1^{-1}u_1^{-1}+4s^2m^4t_1^{-2}u_1^{-2})]\bar{s}^{-1}\ln x \\
&\quad-\{1-\tfrac{1}{2}(3s^2-8m^4)t_1^{-1}u_1^{-1} \\
&\qquad-[5s-12m^2-\tfrac{1}{2}st_1^{-1}u_1^{-1}(3s^2+10sm^2-24m^4)+8s^2m^4(s-2m^2)t_1^{-2}u_1^{-2}]\bar{s}^{-1}\}\ln^2 x \\
&\quad-2[1-(27s-32m^2)t^{-1}+(4s^2-22sm^2+15m^4)t^{-2}+6(5s-4m^2)t_1^{-1}-4m^2(s-4m^2)t_1^{-2} \\
&\qquad+2(13s^2-18sm^2+8m^4)t_1^{-1}u_1^{-1}-2(11s^2-18sm^2+8m^4)t^{-1}u_1^{-1} \\
&\qquad+2(2s^3-13s^2m^2+18sm^4-8m^6)t^{-2}u_1^{-1}]\ln\left[\frac{-t_1}{m^2}\right] \\
&\quad-4[s-(s+2m^2)(s-4m^2)t_1^{-1}-2(s^3-12sm^4+8m^6)t_1^{-1}u_1^{-1} \\
&\qquad+8m^4(s-2m^2)t_1^{-2}]\ln x\ln\left[\frac{-t_1}{m^2}\right]\bar{s}^{-1} \\
&\quad+4[1-(s+4m^2)t_1^{-1}-2m^4t_1^{-2}+2sm^4t_1^{-3}-2(s^2+sm^2-3m^4)t_1^{-1}u_1^{-1}]\mathrm{Li}_2\left[\frac{t}{m^2}\right] \\
&\quad-8(s-2m^2)[2-s(s+4m^2)t_1^{-1}u_1^{-1}+4s^2m^4t_1^{-2}u_1^{-2}][\ln x\ln(1-x)+\mathrm{Li}_2(x)]\bar{s}^{-1} \\
&\quad-2(s-4m^2)[2+s(s+2m^2)t_1^{-1}u_1^{-1}][\ln x\ln(1+x)+\mathrm{Li}_2(-x)]\bar{s}^{-1}\,, \qquad \text{(D3)}
\end{aligned}
$$

with the same definitions as above.

*Present address: Centre de Physique Théorique, CNRS Luminy, case 907 F-13288 Marseille, CEDEX 09, France.

[1]For reviews, see E. L. Berger, Argonne Report No. ANL-HEP-CP-88-26, to be published in the Proceedings of the Advanced Research Workshop on QCD Hard Hadronic Processes, St. Croix, 1987; N. W. Reay, in *Multiparticle Dynamics, 1985,* proceedings of the XVI International Symposium, Kiryat Anavim, Israel, edited by J. Grunhaus (World Scientific, Singapore, 1985); C. Caso, in *Proceedings of the 1985 International Symposium on Lepton and Photon Interactions at High Energies,* Kyoto, Japan, 1985, edited by M. Konuma and K. Takahashi (RIFP, Koyoto, 1986); A. Kernan and G. VanDalen, Phys. Rep. **106**, 298 (1984).

[2]C. Albajar *et al.*, Phys. Lett. B **213**, 405 (1988); C. Albajar *et al.*, Z. Phys. C **37**, 489 (1988); **37**, 505 (1988); M. G. Catanesi *et al.*, Phys. Lett. B **187**, 431 (1987); J. P. Albanese *et al.*, Phys. Lett. **158B**, 186 (1987).

[3]A. Ali, B. van Eijk, and I. ten Have, Nucl. Phys. **B291**, 1 (1987); UA1 Collaboration, C. J. Albajar *et al.*, Z. Phys. C **37**, 489 (1988); Phys. Lett. B **186**, 237 (1987).

[4]A. Ali, in *Physics at LEP,* LEP Jamboree, Geneva, Switzerland, 1985, edited by J. Ellis and R. Peccei (CERN Report No. 86-02, Geneva, 1986); G. Altarelli and P. J. Franzini, Z. Phys. C **37**, 271 (1988).

[5]M. Kobayashi and K. Maskawa, Prog. Theor. Phys. **49**, 652 (1973).

[6]P. Mazzanti and S. Wada, Phys. Rev. D **26**, 602 (1982).

[7]S. J. Brodsky, J. C. Collins, S. D. Ellis, J. F. Gunion, and A. H. Mueller, in *Proceedings of the Summer Study on the Design and Utilization of the Superconducting Super Collider,* Snowmass, Colorado, 1984, edited by R. Donaldson and J. Morfin (Division of Particles and Fields of the APS, New York, 1985).

[8]J. C. Collins, D. E. Soper, and G. Sterman, Nucl. Phys. **B263**, 37 (1986).

[9]R. J. N. Phillips, in *New Particles 1985,* proceedings, Madison, Wisconsin, 1985, edited by V. Barger, D. Cline, and F. Halzen (World Scientific, Singapore, 1986).

[10]M. Gluck, J. F. Owens, and E. Reya, Phys. Rev. D **17**, 2324 (1978); B. L. Combridge, Nucl. Phys. **B151**, 429 (1979); J. Babcock, D. Silvers, and S. Wolfram, Phys. Rev. D **18**, 162 (1978); K. Hagiwara and T. Yoshino, Phys. Lett. **80B**, 282 (1979); L. M. Jones and H. Wyld, Phys. Rev. D **17**, 782 (1978); H. Georgi *et al.*, Ann. Phys. (N.Y.) **114**, 273 (1978).

[11]G. Matthiae, Riv. Nuovo Cimento **4**, 1 (1981).

[12]R. K. Ellis and J. C. Sexton, Nucl. Phys. **B269**, 445 (1986).

[13]P. Nason, S. Dawson, and R. K. Ellis, Nucl. Phys. **B303**, 607 (1988).

[14]G. Altarelli, M. Diemoz, G. Martinelli, and P. Nason, Nucl. Phys. **B308**, 724 (1988).

[15]Z. Kunszt and E. Pietarinen, Nucl. Phys. **B164**, 45 (1980).

[16]F. Halzen and G. Herzog, Phys. Rev. D **30**, 2326 (1984); F. Halzen and P. Hoyer, Phys. Lett. **154B**, 324 (1985); V. Barger and R. J. N. Phillips, Phys. Rev. D **31**, 215 (1985); A. Ali and G. Ingelman, Phys. Lett. **156B**, 111 (1985); G. Kopp, J. H. Kuhn, and P. Zerwas, *ibid.* **153B**, 315 (1985).

[17]J. F. Gunion and Z. Kunszt, Phys. Lett. B **178**, 296 (1986).

[18]L. M. Brown and R. P. Feynman, Phys. Rev. **85**, 231 (1952); I. Harris and L. M. Brown, *ibid.* **105**, 1656 (1957); F. A. Berends and R. Gastmans, Nucl. Phys. **B61**, 414 (1973).

[19]G. 't Hooft and M. Veltman, Nucl. Phys. **B44**, 189 (1972); C. G. Bollini and J. J. Giambiagi, Phys. Lett. **40B**, 566 (1972); W. J. Marciano, Phys. Rev. D **12**, 3861 (1975).

[20]T. Kinoshita, J. Math. Phys. **3**, 650 (1960); T. D. Lee and M. Nauenberg, Phys. Rev. **133**, B1549 (1964); N. Nakanishi, Prog. Theor. Phys. **19**, 159 (1958); H. D. Politzer, Nucl. Phys. **B129**, 301 (1977); C. T. Sachrajda, Phys. Lett. **73B**, 185 (1978); D. Amati, R. Petronzio, and G. Veneziano, Nucl. Phys. **B140**, 64 (1978); **B146**, 29 (1978); R. K. Ellis *et al.*, *ibid.* **B152**, 285 (1979); **B152**, 285 (1979); S. B. Libby and G. Sterman, Phys. Lett. **78B**, 618 (1978); J. C. Collins and G. Sterman, Nucl. Phys. **B185**, 172 (1982); J. C. Collins, D. E. Soper, and G. Sterman, Phys. Lett. **134B**, 263 (1984); Nucl. Phys. **B261**, 104 (1985); G. T. Bodwin, Phys. Rev. D **31**, 2616 (1985).

[21]SCHOONSCHIP is an algebraic-manipulation program written by M. Veltman: see H. Strubbe, Comput. Phys. Commun. **8**, 1 (1974).

[22]J. C. Taylor, Nucl. Phys. **B33**, 436 (1971); A. A. Slavnov, Theor. Math. Phys. **10**, 99 (1972).

[23]G. Passarino and M. Veltman, Nucl. Phys. **B160**, 151 (1979).

[24]W. L. van Neerven, Nucl. Phys. **B268**, 453 (1986).

[25]Many four-dimensional integrals are listed in the thesis of A. N. J. J. Schellekens, Nijmegen University, 1981. Some n-dimensional integrals are listed in A. Devoto, D. W. Duke, J. D. Kimel, and G. A. Sowell, Phys. Rev. D **30**, 541 (1984).

[26]J. Smith. D. Thomas, and W. L. van Neerven, Report No. ITP-SB-87-63 (unpublished).

[27]L. Lewin, *Polylogarithms and Associated Functions* (North-Holland, Amsterdam, 1983).

[28]E. G. Floratos, D. A. Ross, and C. T. Sachrajda, Nucl. Phys. **B129**, 66 (1977); **B139**, 545(E) (1978); **B152**, 493 (1979); A. Gonzales-Arroyo, C. Lopez, and F. J. Yndurain, *ibid.* **B153**, 161 (1979); A. Gonzales-Arroyo and C. Lopez, *ibid.* **B166**, 429 (1980); E. G. Floratos, P. Lacaze, and C. Kounnas, Phys. Lett. **98B**, 89 (1981); **98B**, 285 (1981).

[29]J. Kubar André and F. E. Paige, Phys. Rev. D **19**, 221 (1978); B. Humpert and W. L. van Neerven, Nucl. Phys. **B184**, 225 (1981).

[30]P. Aurenche, R. Baier, M. Fontannaz, and D. Schiff, Nucl. Phys. **B297**, 661 (1988), and references therein

[31]A. H. Mueller and P. Nason, Phys. Lett. **156B**, 226 (1985); Nucl. Phys. **B266**, 265 (1986).

[32]G. A. Schuler, S. Sakakibara, and J. G. Korner, Phys. Lett. B **194**, 125 (1987).

[33]E. J. Eichten, I. Hinchliffe, C. Quigg, and K. D. Lane, Rev. Mod. Phys. **56**, 579 (1984); **58**, 1065(E) (1986).

[34]G. P. Lepage, J. Comput. Phys. **27**, 192 (1978).

[35]R. K. Ellis, M. A. Furman, H. E. Haber, and I. Hinchliffe, Nucl. Phys. **B173**, 397 (1980).